

The WD40 domain-containing protein Ehd5 positively regulates flowering in rice (*Oryza sativa*)

Xuening Zhang ^{1,2,†} Qi Feng ^{1,*†} Jiashun Miao ¹ Jingjie Zhu ¹ Congcong Zhou ¹
Danlin Fan ¹ Yiqi Lu ¹ Qilin Tian ¹ Yongchun Wang ¹ Qilin Zhan ¹ Zi-Qun Wang ¹
Ahong Wang ¹ Lei Zhang ¹ Yingying Shangguan ¹ Wenjun Li ¹ Jiaying Chen ¹ Qijun Weng ¹
Tao Huang ¹ Shican Tang ¹ Lizhen Si ¹ Xuehui Huang ³ Zi-Xuan Wang ^{1,*} and Bin Han ^{1,*}

- 1 National Center for Gene Research, State Key Laboratory of Plant Molecular Genetics, Center of Excellence in Molecular Plant Sciences, Institute of Plant Physiology and Ecology, Chinese Academy of Sciences, Shanghai 200233, China
- 2 University of Chinese Academy of Sciences, Beijing 100049, China
- 3 College of Life Sciences, Shanghai Normal University, Shanghai 200234, China

*Author for correspondence: bhan@ncgr.ac.cn (B.H.), zwxwang@ncgr.ac.cn (Z-X.W.), qfeng@ncgr.ac.cn (Q.F.)

†These authors contributed equally to this work.

The author responsible for distribution of data and materials integral to the findings presented in this article in accordance with the policy described in the Instructions for Authors (<https://academic.oup.com/plcell/pages/General-Instructions>) is: Qi Feng (qfeng@ncgr.ac.cn)

Abstract

Heading date (flowering time), which greatly influences regional and seasonal adaptability in rice (*Oryza sativa*), is regulated by many genes in different photoperiod pathways. Here, we characterized a heading date gene, *Early heading date 5* (*Ehd5*), using a modified bulked segregant analysis method. The *ehd5* mutant showed late flowering under both short-day and long-day conditions, as well as reduced yield, compared to the wild type. *Ehd5*, which encodes a WD40 domain-containing protein, is induced by light and follows a circadian rhythm expression pattern. Transcriptome analysis revealed that *Ehd5* acts upstream of the flowering genes *Early heading date 1* (*Ehd1*), *RICE FLOWERING LOCUS T 1* (*RFT1*), and *Heading date 3a* (*Hd3a*). Functional analysis showed that *Ehd5* directly interacts with Rice outermost cell-specific gene 4 (*Roc4*) and Grain number, plant height, and heading date 8 (*Ghd8*), which might affect the formation of *Ghd7*–*Ghd8* complexes, resulting in increased expression of *Ehd1*, *Hd3a*, and *RFT1*. In a nutshell, these results demonstrate that *Ehd5* functions as a positive regulator of rice flowering and provide insight into the molecular mechanisms underlying heading date.

Introduction

Rice (*Oryza sativa*) is the staple food for more than half of the world's population, and flowering time (or heading date in crops) is one of the most important agronomic traits of rice that determines cultivation distribution and seasonal adaptability (Xue et al. 2008). Flowering is a significant stage in the life cycle of many seed plants, marking the transition from vegetative to reproductive development. Flowering time is influenced by both endogenous genetic pathways and environmental signals such as photoperiod, temperature, and

nutrient availability (Yano and Sasaki 1997; Simpson and Dean 2002; Gao et al. 2013; Zhou et al. 2021) and is crucial for plant adaptation. Therefore, it is essential to investigate the genetic characteristics and molecular regulation networks that govern flowering time, which can facilitate rice genome-guided breeding, variety, improvement, and adaptation.

Photoperiod is an important floral induction factor in plants. Rice is a typical short-day (SD) condition plant whose flowering is induced under SDs and inhibited under long-day (LD) conditions (Itoh et al. 2010). Previous studies have characterized several heading-date-related genes and genetic

Received February 14, 2023. Accepted July 24, 2023. Advance access publication August 30, 2023

© The Author(s) 2023. Published by Oxford University Press on behalf of American Society of Plant Biologists.

This is an Open Access article distributed under the terms of the Creative Commons Attribution-NonCommercial-NoDerivs licence (<https://creativecommons.org/licenses/by-nc-nd/4.0/>), which permits non-commercial reproduction and distribution of the work, in any medium, provided the original work is not altered or transformed in any way, and that the work is properly cited. For commercial re-use, please contact journals.permissions@oup.com

Open Access

regulatory networks associated with flowering in rice. *OsGIGANTEA* (*OsGI*), a homolog of *Arabidopsis* (*Arabidopsis thaliana*) *GIGANTEA* (*GI*), regulates rice flowering time with the change of photoperiod (Hayama et al. 2002). *Heading date 1* (*Hd1*), a homolog of *Arabidopsis* *CONSTANS* (*CO*), works downstream of *OsGI*, promoting rice flowering by increasing *Heading date 3a* (*Hd3a*) expression under SDs (Yano et al. 2000; Kojima et al. 2002; Hayama et al. 2003). *Hd1* has a dual function, promoting heading under SDs and delaying heading under LDs (Yano et al. 2000). *Hd3a* and *RICE FLOWERING LOCUS T 1* (*RFT1*), homologs of *Arabidopsis* *FLOWERING LOCUS T* (*FT*), encode mobile flowering signals and promote floral transition in rice (Komiya et al. 2008). These genes constitute a rice *OsGI-Hd1-Hd3a/RFT1* flowering pathway that corresponds to the *GI-CO-FT* pathway in *Arabidopsis*.

Grain number, plant height, and heading date 7 (*Ghd7*), encoding a CCT (CO, CO-like, and TOC1) domain protein, does not have a homolog in *Arabidopsis* and inhibits flowering under LDs (Xue et al. 2008). *Ehd1*, a rice-specific flowering gene, encodes a B-type response regulator that promotes flowering in both SDs and LDs by upregulating the expression of *Hd3a/RFT1* (Doi et al. 2004; Zhao et al. 2015). These genes form another *Ghd7-Ehd1-Hd3a/RFT1* flowering pathway independent of *Hd1*, with *Ehd1* as the key node of photoperiodic signal integration in rice (Kojima et al. 2002; Doi et al. 2004; Komiya et al. 2008). Meanwhile, *Roc4* which encodes a homeodomain Leu-zipper class IV family protein, and *Ghd8* (also named *DTH8/Hd5*) which encodes a subunit of the CCAAT-box-binding transcription factor HAP3/nuclear transcription factor-YB, can regulate flowering time through affecting *Ehd1* expression under LDs (Wei et al. 2010; Yan et al. 2011; Dai et al. 2012; Wei et al. 2016).

While under LDs, *Hd1* and *Ghd8* interact and form the *Ghd8-Hd1* complex. This complex inhibits the expression of *Hd3a* by increasing its H3K27 trimethylation (H3K27me3) level and activates the transcription of *Ghd7* by binding to its promoter, resulting in late flowering (Du et al. 2017; Wang et al. 2019b). Moreover, previous reports have shown that the *Hd1-Ghd7-Ghd8* combination suppresses the *Ehd1-Hd3a/RFT1* pathway under LDs. *Hd1* also plays a primary positive role in flowering, in competition with the repressive effects of *Ghd7* and/or *Ghd8* under SDs (Cai et al. 2019; Zong et al. 2021; Sun et al. 2022). However, it remains elusive how this inhibition occurs or whether other factors are involved.

The WD40 repeat proteins, which exist widely and are highly conserved in eukaryotes, often fold into a β -propeller structure and provide a platform for protein interaction. They are involved in multiple cellular functions including epigenetic regulation of gene expression, intracellular transport, cell cycle control, chromatin organization, and immune responses (Migliori et al. 2012; Dong et al. 2015; An et al. 2016; Jain and Pandey 2018). In plants, multiple WD40 family proteins have been reported. *Elongator complex subunit 2* (*ELP2*), encoding WD40 repeats containing proteins in *Arabidopsis*, is a subunit that forms the Elongator

complex, along with ELP1 and ELP3-6. The Elongator complex acts as a component of elongating RNA polymerase II holoenzyme in yeast, animals, and plants, and is involved in tRNA modification, DNA modification, and histone acetyltransferase (HAT) activity (Dauden et al. 2017). In rice, *WD repeat domain 5a* (*OsWDR5a*) promotes flowering and panicle development (Jiang et al. 2018). *Salt Responsive WD40 protein 1-5* (*SRWD1-SRWD5*) forms a WD40 subfamily that is involved in salt stress response (Huang et al. 2008). The WD40 family proteins are rich in functions, and their regulatory mechanisms remain poorly understood, so further investigation is needed.

In this study, we identified a rice heading date gene named *Early Heading Date 5* (*Ehd5*). The mutant form of this gene causes rice plants to flower almost 14 days later than the wild-type (WT) plants under both SDs and LDs. The mutation also affects other agronomic traits including grain width, seed setting rates, and grain yield per plant. The *Ehd5* gene is located on rice chromosome 8 and encodes WD40 repeats containing protein. Our research shows that the expression of *Ehd5* gene is regulated by photoperiod and follows a circadian rhythm. It acts upstream of *Ehd1* and *Hd3a/RFT1*. Further studies revealed that *Ehd5* can physically interact with *Roc4* and *Ghd8* in vitro and in vivo, to promote the expression of *Ehd1* and *Hd3a/RFT1* by affecting the formation of *Ghd7-Ghd8* complex. These findings provide insights into the role of WD40 repeat-containing proteins in regulating heading date and promoting flowering in rice by upregulating the expression of *Ehd1* and *Hd3a/RFT1*. Our study enriches the understanding of the genetic regulatory network of flowering-time genes and has potential applications in rice adaptive breeding.

Results

Mutation in *Ehd5* causes late heading in rice

The *ehd5* mutant was isolated from γ -ray-mutagenized M_2 plants of *O. sativa* ssp. *japonica* “Tohoku IL9”. The *ehd5* mutants showed a delayed heading compared to WT IL9 (Fig. 1A). The days to heading of the *ehd5* mutant was 88.3 ± 1.5 days, which was delayed about 12.3 days compared to the wild type (76.0 ± 0.7 days) under natural short-day (NSD) conditions in Hainan, China (Fig. 1B). The heading date of the *ehd5* mutant (86.2 ± 2.1 days) was 15.5 days later than WT plants (68.7 ± 1.6 days) under natural long-day (NLD) conditions in Shanghai, China (Fig. 1C). Both WT and *ehd5* plants flowered after 13 to 14 leaves, with a difference of about 15 days in heading date. Before the flowering of the WT plants, the leaf emergence rate of the *ehd5* plants was 3 to 4 days later than that of the wild type (Supplemental Fig. S1A). Although *Ehd5* had a slight effect on the leaf emergence rate, it controlled mainly the floral transition in rice and not its growth rates. Moreover, we grew the mutants and WT plants in the controlled growth chamber under artificial short-day (ASD) conditions (10-h light/14-h dark) and artificial long-day (ALD) conditions (14-h light/10-h dark). The results were similar to those in the natural field (Supplemental Fig. S1B).

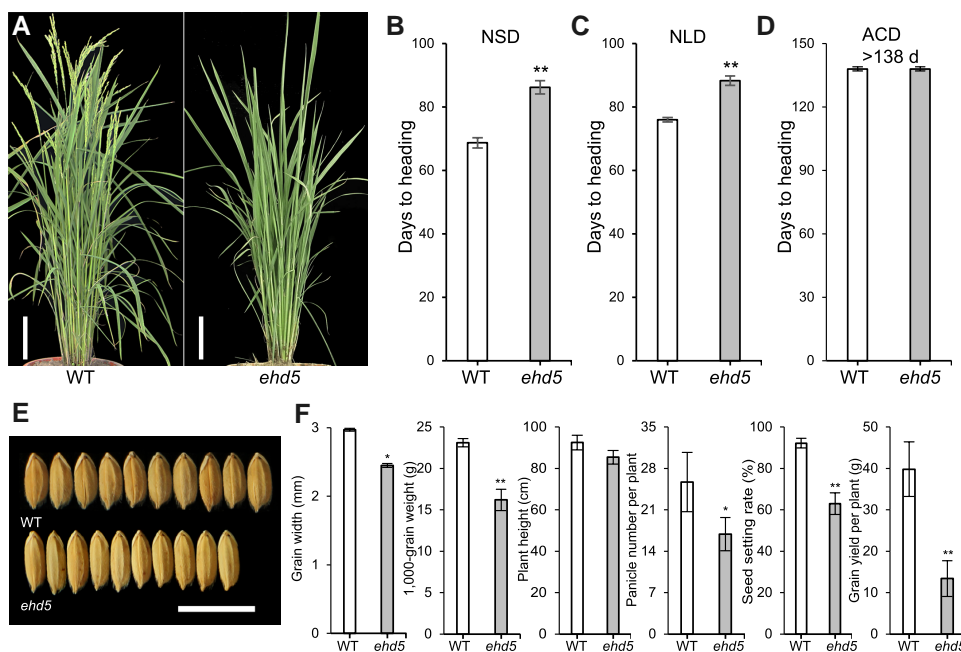


Figure 1. Phenotypes of *ehd5* mutant and wild type (WT) plants. **A)** Flowering phenotypes of 75-d-old WT and *ehd5* plants under NLD conditions. Scale bars =10 cm. **B and C)** Heading date of WT and *ehd5* plants under NSD and NLD conditions. Statistical analysis was conducted on 30 individuals from the wild type and mutant lines. Error bars indicate standard deviations ($n = 30$). ** indicates statistically significant differences: $P < 0.01$ (Student's t test). **D)** Heading date of WT and *ehd5* plants was longer than 138 d under ACD conditions. Error bars indicate standard deviations ($n = 12$). **E)** Grain morphology of WT and *ehd5* plants. Scale bar =1 cm. **F)** Characterization of morphological features of WT and *ehd5* plants. Statistical analysis was conducted on 30 individuals from the wild type and mutant lines. Error bars indicate standard deviations. * indicates statistically significant differences: $P < 0.05$, ** indicates statistically significant differences: $P < 0.01$ (Student's t test). Agronomic traits include grain width, the 1,000-grain weight, plant height, panicle number per plant, seed setting rates, and grain yield per plant.

Interestingly, under artificial continuous day-length (ACD, 24-h light) conditions, the mutant, and WT plants still did not flower even after more than 138 d (Fig. 1D).

The *ehd5* mutant exhibited significant differences in several agronomic traits compared to WT plants. Specifically, the grain width of the *ehd5* mutant was reduced by 17.51% compared to WT, as shown in Fig. 1, E and F. Additionally, the plant height of the *ehd5* mutant showed no significant difference compared to that of WT, and the panicle number per plant was decreased by 34.24% compared to WT (Fig. 1F). Moreover, the *ehd5* mutant showed a significant reduction in grain yield per plant, by 63.82%, and a decrease in seed setting rates by 32.32%. Furthermore, the 1,000-grain weight of the *ehd5* mutant was reduced by 34.20% compared to WT. On the contrary, panicle length and primary branch number of *ehd5* mutant slightly increased compared to wild type (Supplemental Fig. S1, C and D). These results indicated that *Ehd5* promotes flowering under both SD and LD conditions and has a positive effect on yield traits in rice.

Identification of *Ehd5* based on deep sequencing for crossed parents and bulked segregant analysis for F_2 populations

To identify the candidate gene associated with a later heading date, we crossed wild IL9 with an *ehd5* mutant

to generate an F_2 population by self-pollination. The F_2 population contained 756 lines with 572 lines of earlier flowering and 184 lines of later flowering under NSD conditions. It revealed a near segregation ratio of 3:1 ($\chi^2 = 0.1429 < 3.84$), indicating that the phenotype is controlled by a complete monogenic recessive gene. To identify the causal mutation, the F_2 lines were first classified into two bulks based on their heading time, an early heading phenotype group, and a late heading phenotype group. Deep sequencing was performed for both the crossed parents and the pooled extreme wild and mutant phenotypes of the F_2 population. The resulting Illumina sequencing reads were then mapped to the reference rice genome (MSU v7) to detect the causal mutation.

The causative mutation underlying the heading date phenotype was mapped using a newly developed pipeline GradedPool-Seq (Wang et al. 2019a). The mutated gene and its potential effects on gene coding were evaluated according to the gene models of Nipponbare in the RAP-database (DB) annotation system (release 2) of the rice genome (Fig. 2A). Through screening and comparisons between WT and mutant genome sequence, one significant single nucleotide variation (SNV) was found, and then the candidate regions were compared with Rice genome Annotation Database (RAPD, Rice Annotation Project Database). This analysis revealed a region including one open reading frame (ORF), *LOC_Os08g38570*,

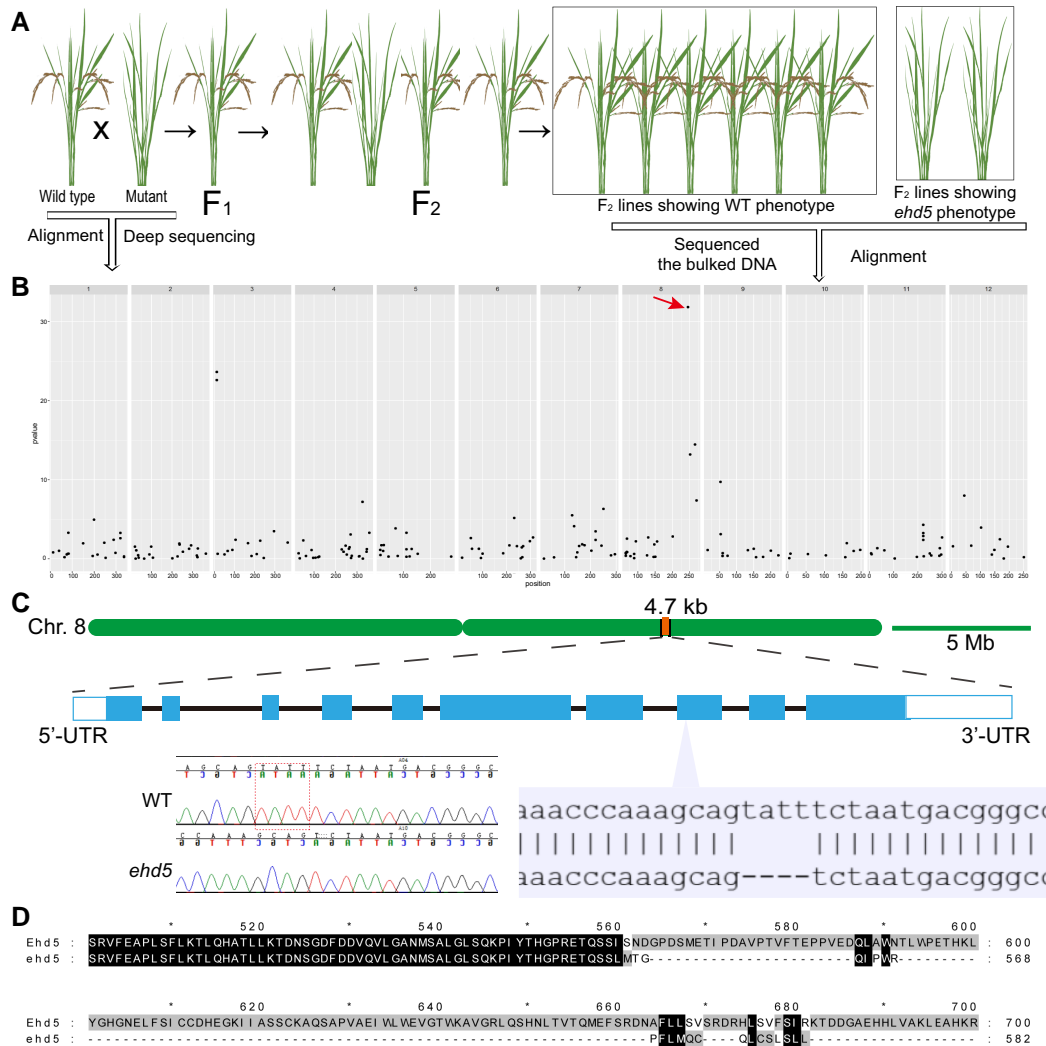


Figure 2. Identification of heading-related gene *Ehd5*. **A**) Identifying the candidate loci by combining deep sequencing of parents and the Bulk Segregant Analysis (BSA) method. IL9 (WT) and late heading mutant were crossed to generate F₂ population that was segregating divided into two phenotyping pools according to the heading date. We sequenced the bulked DNA and aligned it to the reference sequence of Nipponbare (*Japonica*) to calculate *P* values for the single nucleotide polymorphism. The sequencing depths were 100-fold. **B**) The *P* value plot is the result of BSA on the variation tendency of the SNP index between early flowering pool and later flowering pool. The *P* value plot (Y axis) is plotted against SNP positions (X axis) on each of the 12 chromosomes. The down to right arrow on chromosome 8 indicates the candidate loci. **C**) Structure of the *Ehd5* gene. Hollow boxes show the 5' and 3' UTR. Black solid lines and blue solid boxes indicate introns and exons, respectively. The *ehd5* contains a 4-bp deletion (the dashed line box) in the eighth exon. The sequence of trace file comparison of *Ehd5* in WT and *ehd5* was also shown (left). **D**) Amino acids alignment of *Ehd5* protein from IL9 and *ehd5* by using GeneDoc software. The black background represents the identical sequence, while the gray portion indicates the amino acid sequence that does not match.

located on chromosome 8 (Fig. 2B). We named this gene as *Early heading date 5* (*Ehd5*).

The *Ehd5* gene consists of 10 exons and 9 introns and encodes a WD40 repeat protein which is conserved in eukaryotes (Fig. 2C). Gene region sequencing for *ehd5* verified that a 4-bp “tatt” deletion appeared in the eighth exon of *Ehd5* and leads to frameshift mutation (Fig. 2C). This deletion results in premature termination of translation of the *Ehd5* protein, which indicates that *ehd5* is a loss-of-function allele (Fig. 2D).

Complementation and overexpression of *Ehd5* in *ehd5* plants recovers the wild-type phenotype

To confirm whether the variation of *Ehd5* gene was responsible for the *ehd5* phenotypes, we constructed a complementation vector containing the candidate gene and then transformed it into the *ehd5* mutant. In total, 12 positive complementation transgenic plants (*Ehd5*-complementary plasmid [CP]/*ehd5*) were obtained. As observed, the heading date of *Ehd5*-CP/*ehd5* was 10 d earlier than *ehd5* but slightly delayed compared to that of the WT under NSDs

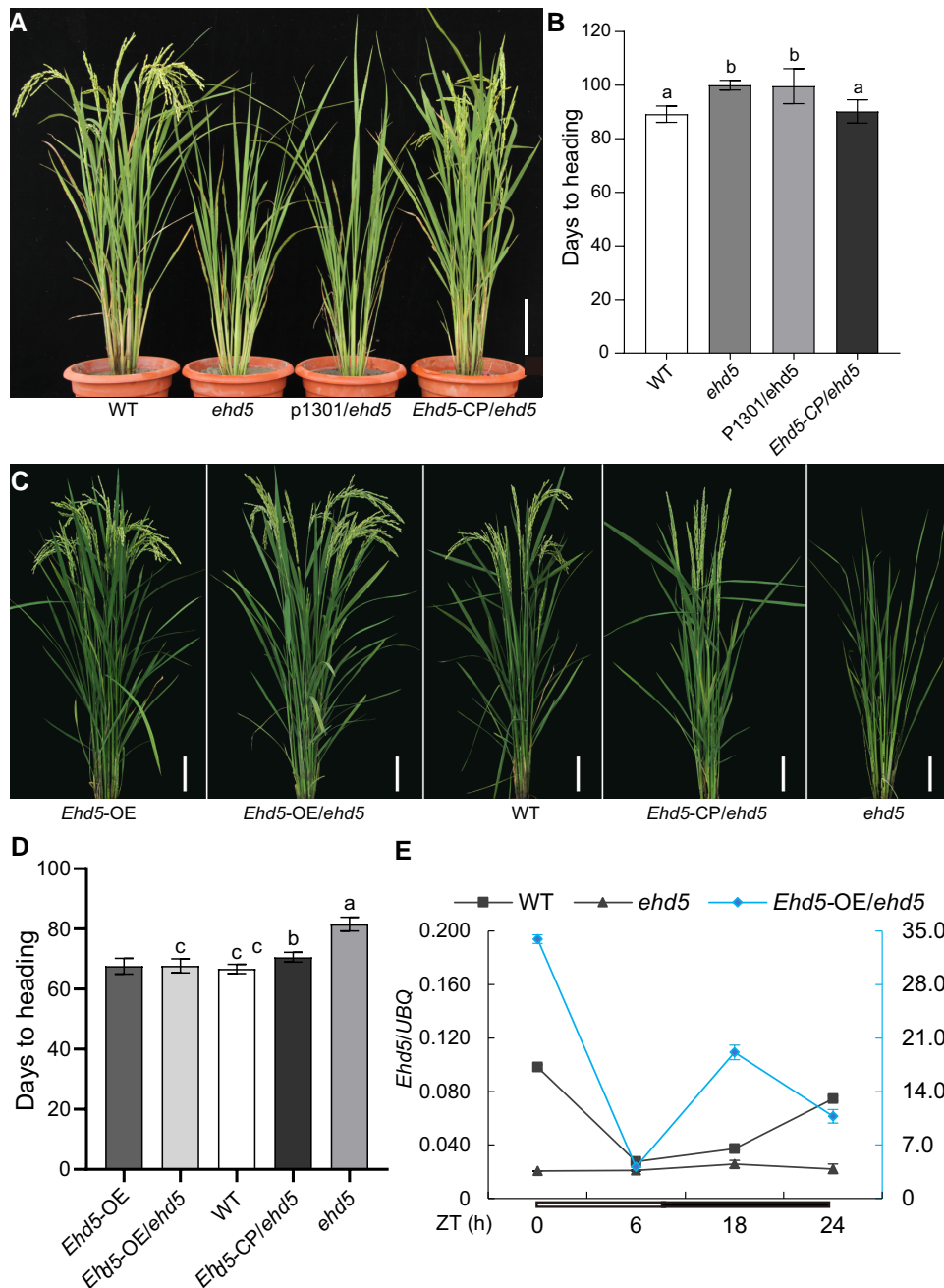


Figure 3. Function verification of *Ehd5* by genetic complementation and overexpression. **A**) Flowering phenotypes of 95-d-old IL9 (WT), *ehd5*, *ehd5* with empty pCambia1301 (*p1301/ehd5*) and *Ehd5* complemented transgenic line (*Ehd5-CP/ehd5*) under NSD conditions. Scale bar = 15 cm. **B**) Heading date statistics of WT, *ehd5*, *p1301/ehd5*, and *Ehd5-CP/ehd5* under NSD conditions. Statistical analysis was conducted on 30 individuals from each line ($n = 30$). Different letters indicate significant differences ($P < 0.05$), as determined by one-way analysis of variance (ANOVA) with Tukey's multiple comparison test. **C**) Flowering phenotypes of 80-d-old WT, *ehd5*, *Ehd5-CP/ehd5*, and *Ehd5* overexpression lines (*Ehd5-OE*, *Ehd5-OE/ehd5*) under NLD conditions. Scale bars = 5 cm. **D**) Heading date statistics of 30 individuals of WT, *ehd5*, *Ehd5-CP/ehd5*, *Ehd5-OE*, and *Ehd5-OE/ehd5* under NLD conditions ($n = 30$). **E**) RT-qPCR analysis of *Ehd5* expression in WT, *Ehd5-OE/ehd5*, and *ehd5* plants under ASD conditions. The hollow line indicates light conditions, the heavy line indicates dark conditions at the bottom. Each time point represents the mean \pm SD of three independent samples. *Ubiquitin* was used to normalize gene expression.

(Fig. 3, A and B). Moreover, we constructed the overexpression vectors of *Ehd5* and transformed the WT and *ehd5* mutant. Both the days to heading of the *proUbi:Ehd5* transgenic lines of wild type (*Ehd5*-overexpressed [OE]) and mutant

(*Ehd5-OE/ehd5*) showed no significant differences compared to that of wild type (Fig. 3, C and D).

We further examined the agronomic phenotypes of *Ehd5*-OE, *Ehd5-OE/ehd5*, WT, *Ehd5-CP/ehd5*, and *ehd5*, such

as the plant height, panicle number per plant, seed setting rates, and grain yield per plant. The results showed these phenotypes of transgenic lines did not differ from the WT but were significantly different from *ehd5* (Supplemental Fig. S2, A to D). Moreover, scanning electron microscopy showed that the grain morphology of *Ehd5*-CP/*ehd5* was completely restored (Supplemental Fig. S3A). The observations of the outer glume surface showed no significant differences in the single cell length, the single cell width, and the total cell number per unit area between WT and *ehd5* plants (Supplemental Fig. S3, B to D). The longitudinal cell number of *ehd5* was reduced by 21.25% compared with that in WT, but cell numbers in *ehd5* lemmas did not differ from that in the WT lemmas in transverse directions (Supplemental Fig. S3, E and F), suggesting that *Ehd5* may regulate grain width by altering cell division.

Similarly, the comparison of grain length and width of *Ehd5*-OE, *Ehd5*-OE/*ehd5*, WT, *Ehd5*-CP/*ehd5*, and *ehd5* plants showed that only the grain width of *ehd5* reduced appreciably compared to the other genotypes (Supplemental Fig. S4, A to E). Furthermore, the *Ehd5* expression level of *Ehd5*-OE/*ehd5* plants was substantially higher than that in WT, and *ehd5* lines displayed reduced *Ehd5* transcript levels (Fig. 3E). Overall, the *Ehd5* gene can promote flowering in rice under both LD and SD conditions, as well as increasing tillering and yield.

Characterization of Ehd5 protein

The predicted Ehd5 protein contains 849 amino acids, with 8 WD40 domains, and shares 58% identity with ELP2 (Supplemental Fig. S5A), which is an epigenetic regulator that regulates disease resistance-related genes such as *NONEXPRESSOR OF PATHOGENESIS-RELATED GENES1* (*NPR1*) to induce immunity in Arabidopsis (Wang et al. 2013). We transiently expressed a green fluorescent protein (GFP)-tagged Ehd5 fusion protein in rice protoplasts under the control of the constitutive cauliflower mosaic virus (CaMV) 35S promoter, with mCherry-NLS (Nuclear Location Signal) fusion protein. Meanwhile, we also co-transformed Ehd5-GFP and the membrane-localization-marker mCherry-MCA in *Nicotiana benthamiana* leaves.

Confocal microscopy showed that the GFP signal was predominantly detected in the cytoplasm and plasma membrane (Fig. 4A, Supplemental Fig. S5B). In addition, we confirmed that Ehd5 localized in the nuclear membrane by co-expressing nuclear-membrane-localization-marker yellow fluorescent protein (YFP)-PNET1 fusion protein and mCherry-Ehd5 in *Nicotiana benthamiana* epidermal cells (Supplemental Fig. S5B). Homology searches and subsequent phylogenetic analysis of Ehd5 protein showed that the amino acid sequence of Ehd5 was conserved in both dicots and monocots, suggesting that the gene is highly conserved, and the homology of monocotyledonous plants is highly similar to that of *Brachypodium distachyon* (Fig. 4B).

In addition, we selected 162 divergent accessions from the pan-genome dataset of the *O. sativa*–*O. rufipogon* species complex (Huang et al. 2012; Zhao et al. 2018) and

constructed a phylogenetic tree using neighbor-joining tree with 1,000 replicates bootstrap. The phylogenetic tree separated *O. sativa* and *O. rufipogon* Ehd5 into different clades (Supplemental Fig. S6A). SNP-seek was performed on the 4747-bp *Ehd5* DNA sequence using the rice 3 K genome database (<https://snpseek.irri.org>). The results showed that only 15 SNPs were found and a total of 3 haplotypes based on these variations were generated (Supplemental Table S1, Supplemental Fig. S6B).

Among these variations, 5 SNPs were located in the intron regions, 3 SNPs were located in the 3'-untranslated regions (UTR) regions, and 7 SNPs occurred on exons, including 2 synonymous mutations and 5 missense mutation SNPs (Supplemental Data Set S1). Those nonsynonymous mutations were found in fewer varieties, and their functions and effects for heading date need to be further explored. In addition, the allele frequencies of 14 SNPs were fixed among different rice varieties, while the allele frequency of one occurring in an intron was 50% in *Tropical japonica* (Supplemental Fig. S6C). Therefore, we inferred that *Ehd5* is not a gene influenced by human selection during domestication and is highly conserved in rice.

To further explore the function of the Ehd5 protein, we performed Weighted Gene Co-expression Network Analysis (WGCNA) based on 52 RNA sequencing (RNA-seq) datasets obtained from 33-d-old leaves from WT and *ehd5* (Supplemental Data Set S2). After filtering out weakly expressed genes, a collection of highly expressed genes was obtained, and sample clustering and module division were performed based on gene expression levels (Supplemental Fig. S7, A and B). The divided modules were associated with traits, resulting in 30 co-expressed gene modules (Supplemental Fig. S7, C and D).

The Gene Ontology (GO) functional enrichment analysis of the gene module containing *Ehd5* revealed that the molecular function (MF) category significantly enriched (false discovery rate < 0.05) GO terms were related to transport activity and binding activity (Fig. 4E). Significantly enriched (false discovery rate < 0.05) GO terms in biological process (BP) category were related to transport, establishment of localization and post-transcriptional modification of protein (Fig. 4D). The significantly enriched (false discovery rate < 0.05) GO terms in cellular component (CC) imply these processes may occur on the cell membrane (Fig. 4C). These findings are consistent with the results of the subcellular localization assay for Ehd5, which identified the Ehd5 protein was located in the cytoplasm, nuclear membrane, and plasma membrane.

Spatiotemporal expression of Ehd5

In order to investigate the spatial- and temporal-transcription patterns of *Ehd5* in various tissues and at different stages of leaf development, reverse transcription quantitative PCR (RT-qPCR) analysis, and glucuronidase (GUS) staining experiments were carried out. At 33 days after germination (DAG), the leaves, around the shoot apex (ASA), sheaths, stem and

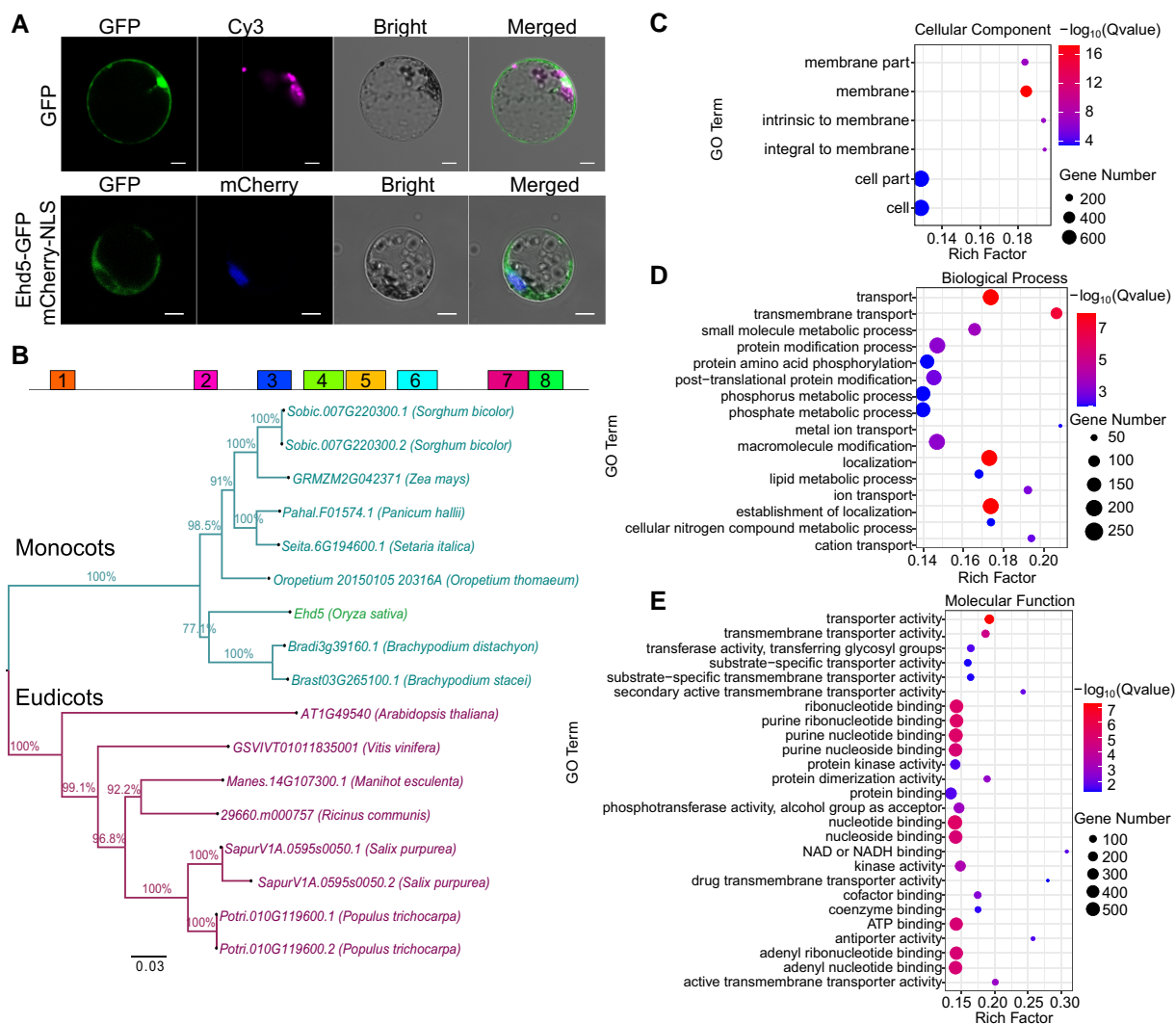


Figure 4. Characterization of Ehd5 protein. **A**) Subcellular localization of Ehd5-GFP fusion protein in rice protoplasts. GFP signal, nucleus-mCherry signal, brightfield, and merged micrographs were shown. The *pro35S::GFP* and *mCherry-NLS* plasmids were used as the control. Bars = 10 μm . **B**) Phylogenetic tree analysis of Ehd5 and its homologous genes in various species. Protein structural analysis showed that Ehd5 protein contains 8 WD40 domains (colorful boxes). The phylogenetic tree was performed using the neighbor-joining method with 1,000 replicates bootstrap by MEGA, and monocotyledons and dicotyledons were clustered separately. Scale bar, the evolutionary distance. The number 0.03 below the scale bar indicates that the length represents a genetic divergence of 0.03 in the genome. **C-E**, GO Enrichment analysis of RNA-Seq showed that representative MF of Ehd5 protein was transport and binding, which mainly occurred in cytoplasm and cell membrane.

roots were collected from WT IL9 grown under ASD (10-h light/14-h dark) and ALD (14-h light/10-h dark) conditions for mRNA isolation. We found that the expression levels of Ehd5 were the highest in the expanding leaf (DL2), while the expression level was low in the root and sheath (Fig. 5, A to C), and this demonstrated that Ehd5 transcripts accumulated most abundantly in developing leaf tissues.

At 23 DAG, we took up to collect the second complete leaf of 3-leaf rice seedlings grown under ASD conditions for the first time and then kept sampling every 5 d until flowering. The results showed that the expression levels of Ehd5 were high at the seedling stage, especially at the panicle primordium differentiation stage, with the highest expression level (Fig. 5D). The expression of Ehd5 declined after the flowering

transition, indicating the importance of Ehd5 in rice flowering.

Then we collected leaf samples every four hours from 33-d-old plants grown under ASD and ALD conditions for 48 h. In the WT plants, the expression of Ehd5 started to increase after dusk and reached a peak at dawn, subsequently it gradually decreased under ASD conditions (Fig. 5E). There was a similar expression pattern under ALD conditions, but the peak of expression level appeared earlier (Fig. 5F). Consistent with those in WT, the expression level in the *ehd5* mutant had similar circadian rhythm, but the expression level was very low all day, possibly as a result of premature termination of transcription (Fig. 5, E and F). The results revealed that the expression of Ehd5 follows a circadian rhythm.

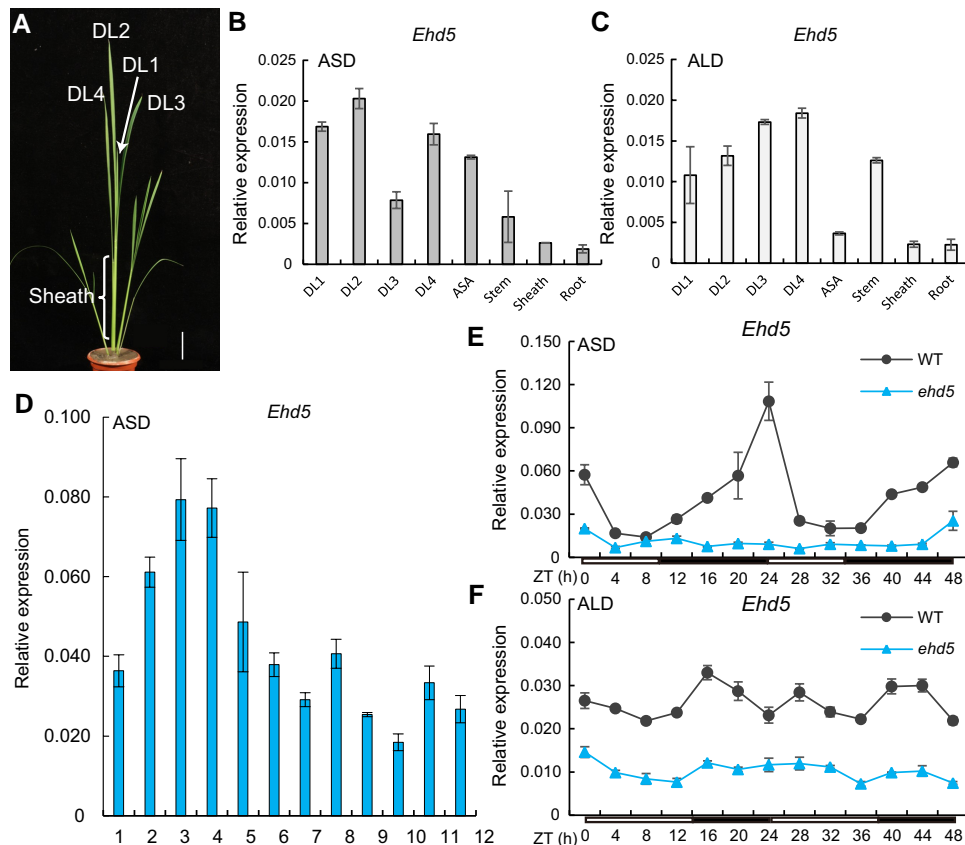


Figure 5. Spatiotemporal expression patterns of *Ehd5*. **A)** Samples from 33-d-old IL plants (WT) grown under ASD conditions. DL1, newly emerging leaf; DL2, expanding leaf; DL3 and DL4, fully expanded leaf. Scale bar = 5 cm. **B)** The relative expression levels of *Ehd5* in different plant tissues under ASD conditions. ASA, around the shoot apex. **C)** The relative expression levels of *Ehd5* in different plant tissues under ALD conditions. **D)** Developmental expression of *Ehd5*. Leaf samples were collected at dawn under ASD conditions. The sampling interval was 5 d from 23 d after germination to the beginning of heading. The numbers on the X-axis represent the sampling iterations. One represents the first sampling, 2 represents the second sampling, and so on. **E)** Rhythmic expression pattern of *Ehd5* in WT and *ehd5* plants under ASD conditions. **F)** Rhythmic expression pattern of *Ehd5* in WT and *ehd5* plants under ALD conditions. The hollow lines indicate light conditions, the heavy lines indicate dark conditions at the bottom. *Ubiquitin* was used to normalize gene expression. Each time point represents the mean \pm SD of 3 independent samples.

Moreover, we generated the *proEhd5:GUS* transgenic plants and observed the expression of *Ehd5* in developing panicles. The strong β -glucuronidase (GUS) activity was detected in young leaf, flower primordia, panicles \sim 1 cm of length, and panicles 10–20 cm of length, which was mainly concentrated in the outer ends of spikelet hulls (Supplemental Fig S8).

Ehd5 physically interacts with Roc4 in vitro and in vivo to promote flowering

To investigate the functional role of *Ehd5* in determining heading date, a yeast 2-hybrid (Y2H) screen was performed. We co-transformed *pGBKT7-Ehd5* and *pGADT7* into yeast-2-hybrid (Y2H) Gold competent cells, and the cells could grow on control medium (SD/-Trp/-Leu) but not on selective medium (SD/-Trp/-Leu/-His or SD/-Trp/-Leu/-His/-Ade), indicating that the gene cannot auto-activate the reporter in yeast (*Saccharomyces cerevisiae*). Then, the *Ehd5* full-length protein was used as the bait and its interacting partners were identified through a Y2H screen.

The C-terminal truncated protein Roc4 was isolated, which has been reported to regulate rice flowering (Wei et al 2016). We confirmed the interaction of *Ehd5* with the full length Roc4 and truncated variant of Roc4 (500 to 814) in yeast cells (Fig. 6A). We conducted a bimolecular fluorescence complementation (BiFC) assay to further verify the interaction between *Ehd5* and Roc4 in plant cells. *Ehd5* and Roc4 were fused with the C and N terminus of the YFP (*Ehd5*-cYFP, ROC4-nYFP), respectively, and then were co-expressed in *Nicotiana benthamiana* leaves. YFP fluorescence was detected in the nucleus, suggesting that *Ehd5* associates with Roc4 in plant cells (Fig. 6B).

Subsequent co-immunoprecipitation (co-IP) experiments in rice protoplasts provided biochemical evidence for the interactions in vivo (Fig. 6C). These results indicate that *Ehd5* can directly interact with Roc4 in vitro and in vivo. Expression analysis of *Roc4* showed that the expression levels of *Roc4* were increased in *Ehd5*-OE/*ehd5* and decreased in *ehd5* plants, compared to those in WT plants, which were consistent with *Ehd5* expression levels in those lines

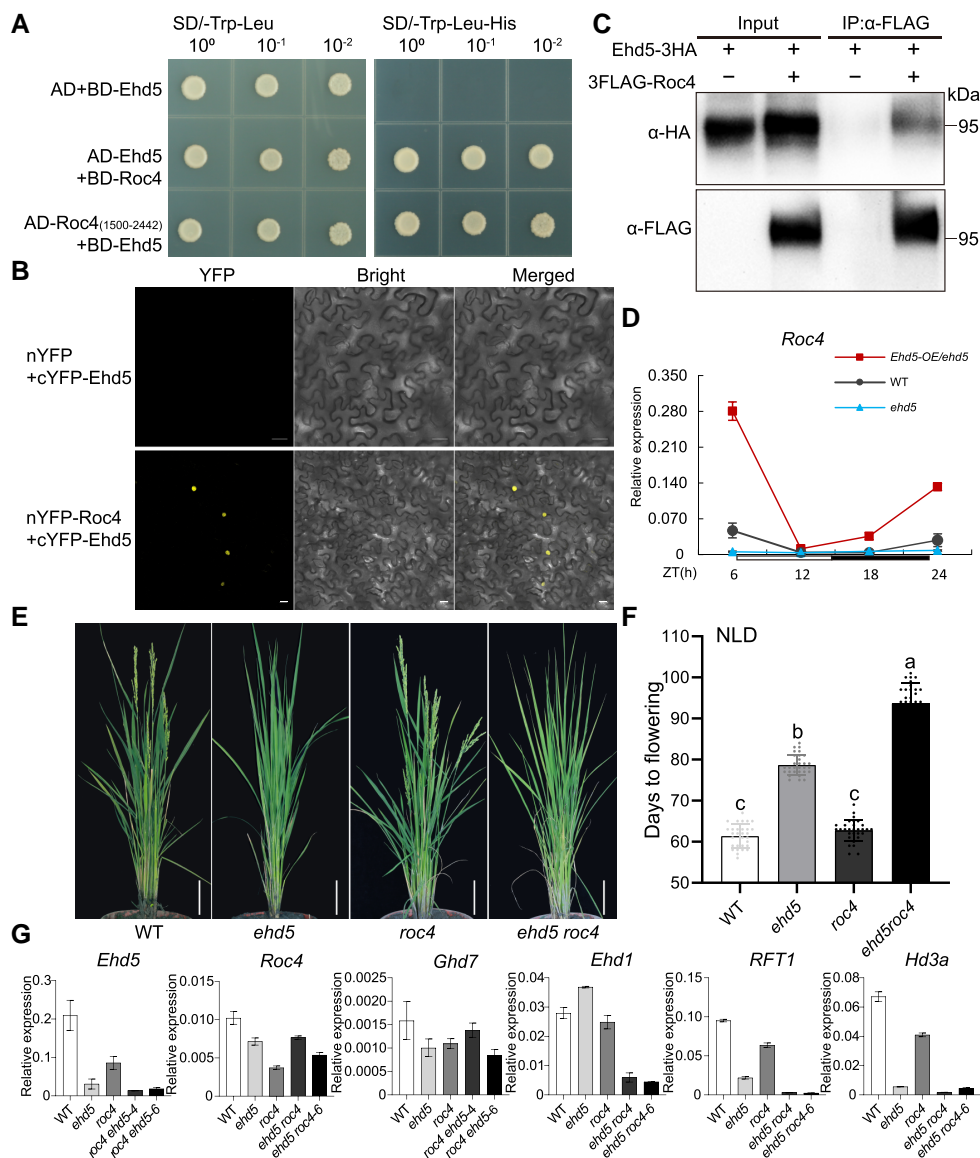


Figure 6. Ehd5 interacts with Roc4 to promote flowering under ALD conditions. **A)** Yeast-2-hybrid (Y2H) assay demonstrating that Ehd5 interacted with Roc4. Yeast cells were grown on SD/-Trp-Leu medium and selective SD/-Trp-Leu-His medium. Binding domain (pGBKT7) and AD (pGADT7) were the bait and prey vectors, respectively. **B)** BiFC showed that the interaction between Ehd5 and Roc4 occurred in the nucleus. Ehd5 and Roc4 were fused with either the C or N terminus of YFP respectively, and then infiltrated into *Nicotiana benthamiana* leaves. Scale bars = 20 μ m. **C)** Co-IP assays in rice protoplasts indicate that Ehd5 interacts with Roc4. The expressed proteins were immunoprecipitated with anti-FLAG beads and detected with anti-HA (HA Peptide, H-Tyr-Pro-Tyr-Asp-Val-Pro-Asp-Tyr-Ala-OH) and anti-FLAG antibodies. The symbols “-” and “+” represent the absence and presence of the corresponding proteins. **D)** Expression analysis of *Roc4* in WT, *Ehd5-OE/ehd5*, and *ehd5* plants under ASD conditions. Hollow line indicates light conditions, heavy line indicates dark conditions at the bottom. Each time point represents the mean \pm SD of three independent samples. *Ubiquitin* was used to normalize gene expression. **E)** Comparison of the phenotypes of IL9 (WT), *ehd5*, CRISPR-CAS9 (Clustered Regularly Interspaced Short Palindromic Repeat-CRISPR-Associated protein 9)-mediated targeted mutagenesis of *Roc4* (*roc4*) and *ehd5 roc4* plants grown under NLD conditions in Shanghai. Scale bars = 10 cm. **F)** Days to flowering of WT, *ehd5*, *roc4*, and *ehd5 roc4* plants under NLD conditions. Statistical analysis was conducted on 30 individuals from each line. Different letters indicate significant differences ($P < 0.05$), as determined by one-way ANOVA with Tukey’s multiple comparison test. **G)** Expression analysis of *Ehd5*, *Roc4*, *Ghd7*, *Ehd1*, *RFT1*, and *Hd3a* in WT, *ehd5*, *roc4*, and *ehd5 roc4* plants under ALD conditions. Each time point represent mean \pm SD of three independent samples.

(Fig. 6D). Therefore, we propose that the expression rhythm of *Roc4* might be affected by the mutation of *Ehd5*.

Given that *Ehd5* and *Roc4* promoted flowering under LD conditions, and that *Ehd5* and *Roc4* interact with each other, we then

knocked out *Roc4* in both WT and *ehd5* plants by using the CRISPR-CAS9 (Clustered Regularly Interspaced Short Palindromic Repeat-CRISPR-Associated protein 9) genome editing system (Ma et al. 2015a, 2015b) and obtained several

homozygous loss-of-function mutant lines (Supplemental Fig. S9). The heading date of *roc4* plants was the same as that of the WT plant, as previously reported (Wei et al. 2016). However, the heading date of the *ehd5 roc4* lines (93.73 d) was later than that of the WT, *ehd5* and *roc4* lines (61.40, 78.67, and 62.73 d, respectively) under NLD conditions (Fig. 6, E and F, Supplemental Data Set S3). Furthermore, the expression levels of *Ehd5*, *RFT1*, and *Hd3a* in *roc4* and *ehd5 roc4* plants were lower than those in WT plants, especially *Ehd1*, *RFT1*, and *Hd3a* transcripts were very low in *ehd5 roc4* plants (Fig. 6G). These results suggested that the interaction between Ehd5 and Roc4 promoted flowering in rice by upregulating the expression of *Ehd1*, *RFT1*, and *Hd3a*.

Ehd5 interacts with Ghd8 and promotes the expression of *Ehd1* and *Hd3a*

To explore the roles of *Ehd5* in the flowering time regulatory network, RNA-Seq was conducted for both WT and *ehd5* mutant samples. A total of 52 leaf samples, with 26 samples collected from WT plants and 26 samples from *ehd5* mutant plants, were obtained every four hours from 33-d-old plants grown under both ASD and ALD conditions for 48 h. Correlation analyses were conducted to study the expression profiles of different flowering-related genes. The results showed the expression profiles of *Ghd8*, *Roc4*, *OsGI*, *MADS-box protein gene; days to heading (OsMADS50)*, *Hd1*, *Phytochrome B (OsPhyB)*, *Ehd1*, and other heading date regulation genes were significantly correlated with the expression of *Ehd5*. Manually checking the expression level of these gene-pairs across 48 h (4 h intervals) confirmed that these correlated gene pairs exhibit similar expression patterns (Supplemental Fig. S10, A and B). Notably, the correlation coefficient between Ehd5 and Ghd8 reached 0.63 under ASD conditions. Therefore, we preliminarily inferred that *Ehd5* may play a role in the regulatory network of heading date.

In order to identify potential up- and down-stream genes related to *Ehd5*, the expression levels of *Ehd5* and other heading-date-related genes including *Ghd8*, *Ghd7*, *Roc4*, *Ehd1*, and *Hd3a* were further quantified using reverse transcription quantitative PCR (RT-qPCR) (Supplemental Fig. S10, C and D). Because *Hd1* from the WT IL9 plants is a defective allele (Matsubara et al. 2008, Matsubara et al. 2011; Zong et al. 2021), we omitted the analysis of *Hd1* in subsequent quantitative experiments. Under both ASD and ALD conditions, the expression levels of *Ehd1* and *Hd3a* in *ehd5* were lower than in WT, suggesting that *Ehd1* and *Hd3a* act downstream of *Ehd5* in the regulation of flowering in rice (Fig. 7, A to D). However, the peak transcription level of *Ghd8* in *ehd5* was slightly higher than WT (Fig. 7E). While the expression of *Ghd7* gene was not substantially different under ALD conditions (Supplemental Fig. S11A). Similarly, there was no substantial difference in the expression level of *Ehd5* in the near-isogenic line (NIL) pyramiding functional *Ghd7* in the *O. sativa* ssp. *Indica* Zhenshan 97 background and Zhenshan 97 lines (Supplemental Fig. S11B).

Previous studies have shown that genetic interactions and mutual regulation of *Hd1*, *Ghd7*, and *Ghd8* were critical for

the rice heading date (Li et al. 2015; Zhang et al. 2015; Nemoto et al. 2016; Du et al. 2017; Zhang et al. 2017; Wang et al. 2019b; Zhang et al. 2019a, 2019b; Zong et al. 2021). Thus, we explored whether they interacted with Ehd5 at the protein level. A yeast 2-hybrid assay showed that Ehd5 interacted with Ghd8 in yeast (Fig. 7F), but not with Hd1, Ghd7, Ehd1, and Hd3a. Furthermore, a luciferase complementation imaging (LCI) assay in *N. benthamiana* leaves by transiently expressing Ehd5-LUC^C and Ghd8-LUC^N, as well as a BiFC assay (Ehd5-cYFP, Ghd8-nYFP), confirmed the interaction in plant cells (Fig. 7, G and H). Moreover, the interaction between Ghd8 and Roc4 was also confirmed by the Y2H assay, BiFC assays, and LCI assays (Fig. 7, F to H). A Co-IP assay showed that HA (HA Peptide, H-Tyr-Pro-Tyr-Asp-Val-Pro-Asp-Tyr-Ala-OH)-Ehd5 could be co-immunoprecipitated by FLAG-Ghd8 in total extract of rice protoplasts (Fig. 7I). And these results indicate that Ehd5 can directly interact with Ghd8 in vitro and in vivo.

We knocked out *Ghd8* using CRISPR/Cas9 system (Ma et al. 2015a, 2015b) in both WT and *ehd5* mutants and obtained homozygous single-base deletion mutants (Supplemental Fig. S12A). It was observed that the *ghd8 ehd5* plants had substantially delayed heading compared to the WT, and reduced tillering under ALD conditions (Fig. 7J). However, the RT-qPCR results showed that the expression levels of *Ehd1*, *Hd3a*, and *RFT1* were upregulated in the double mutant plants during the floral transition period (Fig. 7K). *Ghd8* is a key floral repressor, that suppresses the *Ehd1-Hd3a/RFT1* pathway by forming repressive complexes with *Hd1* or *Ghd7* under LD conditions (Zhu et al. 2017; Wang et al. 2019b). So, we hypothesize that the loss of function of *Ghd8* is an important reason leading to the upregulation of *Ehd1*, *Hd3a*, and *RFT1* expression in the double mutant lines. Moreover, analysis of RT-qPCR results showed that expression of *Ehd5* and *Roc4* were not affected in *ghd8* mutant, compared with that in *O. sativa* ssp. *japonica* “Dongjing” (Supplemental Fig. S12B). These observations suggested that there is no genetic interaction between *Ehd5*, *Ghd8*, and *Roc4*.

It has been reported that Ghd8 was located in the nucleus and could form a heterotrimeric complex with Ghd7 and Hd1 to repress the expression of *Ehd1* and *Hd3a*. LCI assays showed that Ghd7 weakened the interaction between Ehd5 and Ghd8, and Ehd5 weakened the interaction between Ghd7 and Ghd8 (Fig. 8, A and B). Since the subcellular localization of Ghd8 was in the nucleus and the interaction between Ehd5 and Ghd8 occurs in the cytoplasm (Supplemental Fig. S13A), the Ehd5-mCherry, and Ghd8-GFP were transiently co-expressed in *N. benthamiana* leaves. Four groups of different bacteria ratios were set on the same leaf, and the localization of Ghd8 and Ehd5 was assessed at 48 and 72 h after injection (Supplemental Fig. S13B). The results showed that the ratios of cells exhibiting Ghd8 the nuclear localization were decreased along with the increasing quantity of Ehd5-mCherry plasmids after 48 h of injection and the percentages of Ghd8 nuclear localization were almost zero after 72 h of injection (Fig. 8C, Supplemental Fig. S13C, D). These results demonstrated that

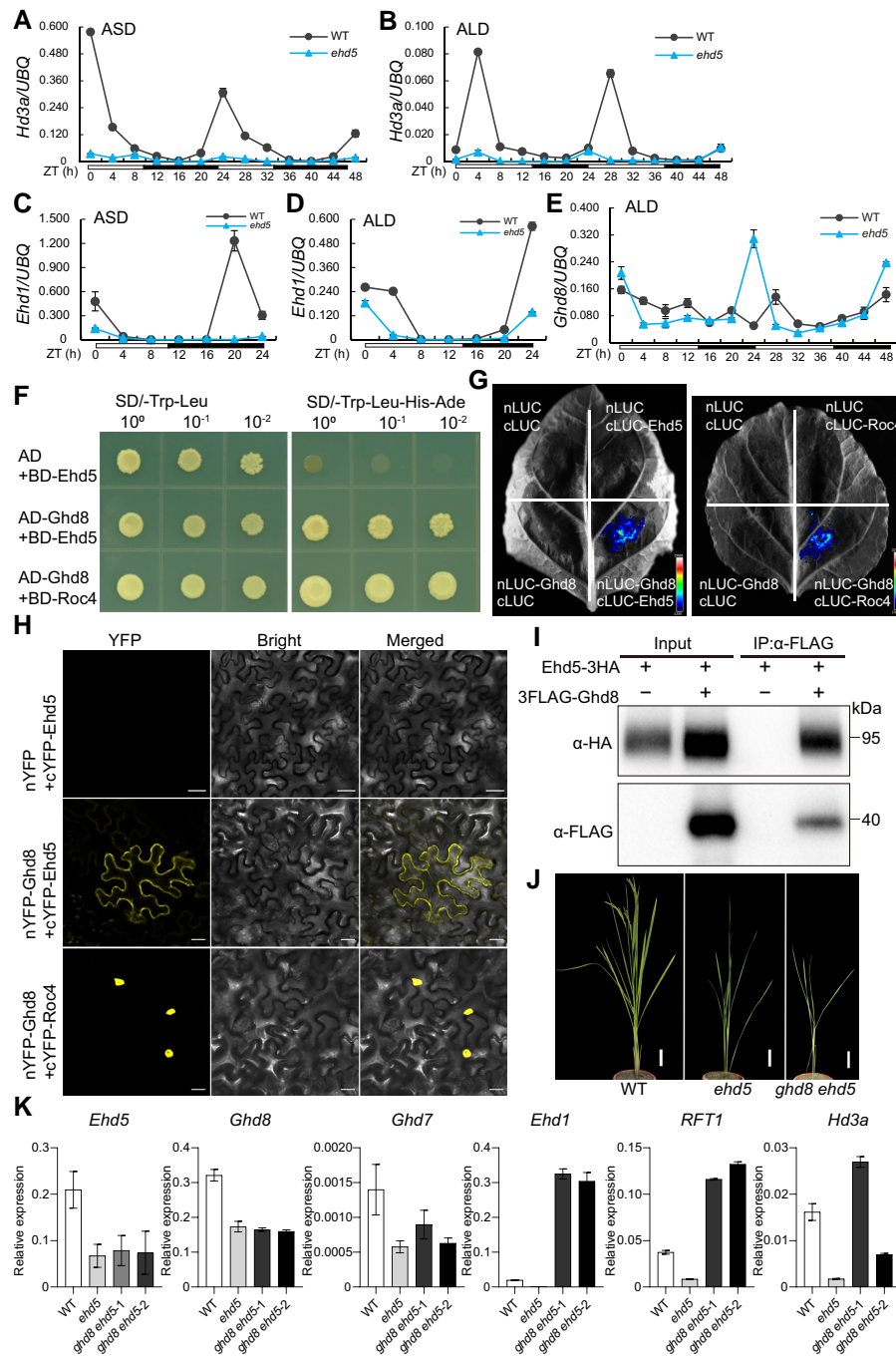


Figure 7. The interactions between Ehd5, Ghd8, and Roc4 regulate the expression of *Ehd1* and *Hd3a*. **A to E**) Rhythmic expression patterns of *Hd3a* (A, B), *Ehd1* (C, D), and *Ghd8* (E) in IL9 (WT) and *ehd5* plants under ASD and ALD conditions. Leaf samples were collected every 4 h from 33-d-old plants. The hollow lines and heavy lines indicate light and dark periods, respectively. Ubiquitin was used to normalize gene expression. Error bars represent SD of 3 independent batches of plants. ZT, the Zeiger Time. ZT = 0 is set to the time of lights on. **F**) Yeast-2-hybrid assays showed the interactions between Ehd5 and Ghd8, Ghd8 and Roc4. **G**) Luciferase luminescence images (LCI) assays of interactions between Ghd8 and Ehd5 or Roc4. The indicated fusion pairs were co-expressed in *N. benthamiana* leaves. The color of the scale indicates increasing intensity from bottom to top. **H**) BiFC assays between Ghd8 fused with N terminus of N-YFP and Ehd5 or Roc4 fused with the C-terminus of YFP (CYFP). Scale bars = 50 or 20 μ m. **I**) *In vivo* interaction between Ehd5 and Ghd8 shown by Co-IP in rice protoplasts. *ProUbi:3 HA (HA Peptide, H-Tyr-Pro-Tyr-Asp-Val-Pro-Asp-Tyr-Ala-OH)-Ehd5* and *pro35S:3 FLAG-Ghd8* were co-expressed in rice protoplasts. Total protein extracts were immunoprecipitated by anti-FLAG beads. The input and co-immunoprecipitated proteins were detected by anti-HA and anti-FLAG antibody. The symbols “-” and “+” represent the absence and presence of the corresponding proteins. **J**) Comparison of the phenotypes of WT, *ehd5*, and CRISPR-CAS9 (Clustered Regularly Interspaced Short Palindromic Repeat-CRISPR-Associated protein 9)-mediated targeted mutagenesis of *Ghd8* in *ehd5* plants grown under ALD conditions. Scale bars = 10 cm. **K**) Expression analysis of *Ehd5*, *Ghd8*, *Ghd7*, *Ehd1*, *RFT1*, and *Hd3a* in WT, *ehd5* and *ghd8 ehd5* plants under ALD conditions. Ubiquitin was used to normalize gene expression. Error bars represent SD of three independent batches of plants.

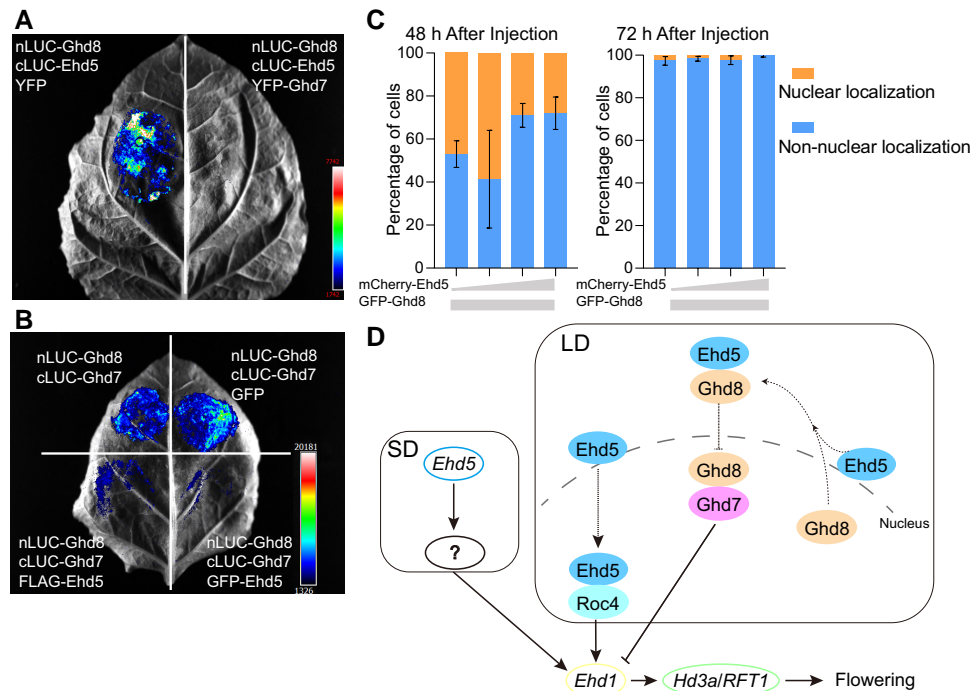


Figure 8. A proposed model for regulating rice flowering by Ehd5. **A)** Luciferase luminescence images (LCI) assays verify that Ghd7 interferes with the interaction between Ehd5 and Ghd8. The color of the scale indicates increasing intensity from bottom to top. **B)** An LCI assay verifies that Ehd5 interferes with the interaction between Ghd8 and Ghd7. Different combinations of reporters and effectors were introduced into *N. benthamiana* leaves. The color of the scale indicates increasing intensity from bottom to top. **C)** The ratios of Ghd8 nuclear localization were gradually reduced along with increasing of *Ehd5* plasmids. And the ratios of Ghd8 nuclear localization were significantly lower after 72 h than after 48 h of injection. Data are presented as mean \pm SD. $n = 3$ independent experiments with 100 cells analyzed for each assay. **D)** The proposed model. Under LD conditions, the Ehd5-Roc4 complexes are localized in the nucleus and promote the expression of *Ehd1*, *Hd3a*, and *RFT1*. For another, Ehd5 can interact with Ghd8, which contributes to the translocation of Ghd8 from the nucleus to cytoplasm. The Ehd5-Ghd8 complexes might affect the formation and function of the Ghd8-Ghd7 complexes, and subsequently promote the expression of *Ehd1* and *Hd3a*. Under SD conditions, *Ehd5* promotes the expression of *Ehd1*, *Hd3a*, and *RFT1*, and there may be other factors involved in this process. Solid line arrows represent a genetic promotion relationship, while dashed line arrows indicate protein import and export from the nucleus.

Ehd5 interacts with Ghd8 and affects the nuclear localization of Ghd8.

Discussion

Heading date is an important agronomic trait for rice breeding, and many heading-date-related genes have been cloned. Previous studies revealed two typical regulatory pathways, an evolutionarily conserved *Hd1-H3a/RFT1* pathway and a rice-specific *Ghd7/Ghd8-Ehd1-Hd3a/RFT1* pathway (Zhou et al. 2021). In this study, we identified a heading-date-related gene *Ehd5*, which promotes rice flowering under both LD and SD conditions, by using the GradedPool-Seq method. Mutants with a loss-of-function of *Ehd5* exhibited delayed flowering compared with the WT, whereas overexpression or complementation of *Ehd5* in *ehd5* plants lead to normal flowering (Fig. 3). Subsequent RNA-seq analysis and RT-qPCR analysis showed *Ehd5* exhibited a circadian rhythm pattern and was induced by light, suggesting that it is involved in rice heading date regulation (Fig. 5, E and F). Furthermore, molecular and biochemical experiments indicated that Ehd5 can form a protein complex with Ghd8

and Roc4, which promotes the expression of *Ehd1* and *Hd3a* under both SD and LD conditions (Figs. 6 and 7). Ehd5 interacts with Ghd8 and affects nuclear localization of Ghd8, as well as there is competitive binding between the Ghd7 and Ehd5 proteins, which means that the Ehd5-Ghd8 protein complex will affect the formation and function of the Ghd8-Ghd7 protein complex (Fig. 8, A to C).

Based on these results and the reported molecular mechanisms, we proposed a molecular model to illustrate the regulatory mechanism of *Ehd5* (Fig. 8D). Under LD conditions, the Ehd5-Roc4 complexes are localized in the nucleus and promote the expression of *Ehd1*, *Hd3a*, and *RFT1*. Meanwhile, Ehd5 interacts with Ghd8 and the Ehd5-Ghd8 complexes are located in the cytoplasm. Therefore, we speculate that there is a competition between Ehd5-Ghd8 heterodimeric complex and Ghd8-Ghd7 complex. However, the processes involved the entry of Ehd5 into the nucleus and the exit of Ghd8 from the nucleus, and more mechanisms need to be further explored. *Ehd5* loss-of-function mutation may facilitate the formation of the Ghd8-Ghd7 complex, which leads to late flowering. Under SD conditions, *Ehd5* promotes the expression of *Ehd1* and *Hd3a/RFT1*, and there may

be other factors involved in this process. The detailed mechanism still needs to be further studied.

Ehd5 is a member of the WD40 protein family, and it has 8 WD40 repeat motifs. In Arabidopsis, *ELP2* can regulate the immune response induced by pathogen responses and abiotic stresses, which is associated with the accumulation of reactive oxygen species (ROS) and salicylic acid (SA), as well as jasmonic acid (JA) and ethylene resistance pathways (Wang et al. 2015; An et al. 2017). Similarly, reduced resistance to bacterial pathogens was observed in *ehd5* mutants in the natural environment (Supplemental Fig. S14, A and B). Subsequently, we inoculated rice blast at the seedling stage and found that *ehd5* mutants were more susceptible compared with WT plants. However, we did not find other Elongator subunits and interactions between Ehd5 and homologous proteins of ELP1 and ELP3-6 in rice.

The structure of ELP2 and Elongator complex in yeast and human have been revealed, which revealed that ELP2 is the core component of this complex and indispensable (Dong et al. 2015; Dauden et al. 2017; Schapira et al. 2017). ELP2 contains two tandemly arranged WD40 repeats while the final β strand deletion of this protein can fail to bind to ELP1 and impaired function of the Elongator complex (Dalwadi and Yip 2018). Here, the structure of Ehd5 in WT and *ehd5* mutant which were predicted online using I-TASSER and Swiss-Prot showed that there was a deletion of the C-terminal β strand in the *ehd5* mutant that might cause a loss function of Ehd5 (Supplemental Fig. S15, A to C). Therefore, the discovery of Ehd5 may provide insight into the regulation mechanism of the Elongator complex in rice.

Heading date is a critical agronomic trait determining the transition from vegetative to reproductive growth, and ultimately affecting the yield and quality of rice (Jung and Müller 2009). SNP-seek results showed *Ehd5* is conserved among rice natural variations and loss-of-function of *Ehd5* results in a significant decrease in seed setting rates, grain yield per plant, plant height, and panicle number per plant, whereas overexpression of *Ehd5* caused an increase of them (Fig. 1, Supplemental Fig. S2). Simultaneously, Ehd5 affects the grain morphology (Supplemental Fig. S3 and S4). Thus, we speculated that *Ehd5* plays pleiotropic roles in regulating grain shape, productivity, and heading date in rice and it has the potential to improve agronomic traits in rice breeding.

In conclusion, we characterized a heading date gene *Ehd5* encoding a WD40 repeat protein that promotes rice flowering under both SD and LD conditions. We propose that *Ehd5* up-regulate the expression of *Ehd1* and *Hd3a* by interacting with Roc4 and Ghd8 or affecting their transcription levels. Although the regulatory mechanism of *Ehd5* has not been thoroughly clarified and the extended function of Ehd5 should be investigated in further detail, our results contribute toward understanding the biological function of WD40 repeat proteins in plants. Moreover, we propose that *Ehd5* may be potentially useful for breeding rice varieties with wider planting areas and higher grain yields.

Materials and methods

Plant materials and growth conditions

In this study, Tohoko IL9 (*Oryza sativa* ssp. *indica*) was used as the wild type and the mutant was selected from the mutant libraries derived from IL9 by radioactive γ -ray, which the same mutant library as the previous study used for *ehd2* (early heading date 2) (Matsubara et al., 2008) and *ehd3* (early heading date 3) (Matsubara et al. 2011). The phenotype of the mutant was similar to that of *ehd2* and *ehd3*. Thus, we named it *ehd5* (early heading date 5) according to the name rules of *ehd2* and *ehd3*. Rice plants were grown in the experimental paddy fields at Chinese Academy of Sciences (CAS) Center for Excellence in Molecular Plant Science in Shanghai (121°42' E, 30°97' N) and in Lingshui (110°18' E, 18°34' N), Hainan Province, China, in different growing seasons. Wild type and *ehd5* mutant plants were grown in the controlled growth chamber (Yiheng Technical Co. Ltd., MGC-350HP) at 26°C, under ASD conditions (10-h light/14-h dark) and ALD conditions (14-h light/10-h dark) with 16,000 Lux illumination intensity from light emitting diode light source and 70% relative humidity. *Nicotiana benthamiana* were cultivated in a chamber maintained at 22 °C under 16 h light conditions. The humidity level was maintained at 60%. Plants grown for 23 to 30 d will be used for subsequent experiments.

DNA extraction and genome sequencing

Genomic DNA (gDNA) was extracted from fresh young leaves of both wild type and *ehd5* mutant plants as well as from each F₂ population, using Hi-DNAsecure Plant Kit following the manufacturer's instructions (Tiangen Biotech, Beijing, China). The gDNA of WT and *ehd5* mutant were fragmented into 500 bp length for Illumina sequencing library construction. The Illumina DNA sequencing libraries were then constructed using the KAPA HyperPrep Kit (Kapa Biosystems, Roche, USA) following the manufacturer's recommendation. Amplification-free approach was employed for library preparation (Kozarewa and Turner 2011), in order to reduce PCR bias and the incidence of duplicate sequences. The bulked gDNA of wild and mutant phenotype F₂ populations were used to prepare for high-throughput sequencing libraries following the same protocol above. All genomic libraries were sequenced on the Illumina HiSeq2500 platform under a paired-end 2 × 150 bp protocol. A total of 52.37 Gb of raw data were generated for two parents and F₂ populations. After quality control by using fastp (version 0.12.6) with default parameters, the clean data was kept for the following data analysis.

Bulked segregant analysis and deep sequencing of parents for identification of candidate gene

To identify the candidate causative gene in *ehd5*, we crossed WT Tohoko IL9 with mutant *ehd5* and generated an F₂ population. By assessing the heading date of each individual progeny, the F₂ lines were divided into two bulks, an early heading phenotype (similar to wild type) group and a late heading phenotype

(similar to *ehd5*) group. We selected 48 individuals from each bulk for whole-genome sequencing. After performing deep sequencing for WT “Tohoku IL9” and *ehd5* mutant, as well as both pooled sequencing for the extreme WT and mutant phenotype of F₂ populations, Illumina sequencing reads of both parents and the pooling samples of F₂ lines were mapped to the reference rice genome (IRGSP4.0) with burrows-wheeler alignment tool (version 0.7.1) to generate the binary alignment/matching files. Duplicated reads generated by PCR were removed using the “markdup” command within SAMtools software. The retained reads were then realigned in the highly polymorphic regions, and the variants (including SNPs and small indels) were further called using the “UnifiedGenotyper” module within the Genome Analysis ToolKit (GATK) and filtered by the base depths (≥ 5). The causative mutation site underlying the heading date was identified using a newly developed pipeline GradedPool-Seq (Wang et al. 2019a). The mutated gene and its potential effects on gene coding were evaluated according to the gene models of Nipponbare in the RAP-DB annotation system (release 2) of the rice genome.

Gene cloning, plasmid construction, and transformation

To generate a complementation plasmid, an 8,891 bp genomic region including 4,144 bp promoter and coding sequence of *Ehd5* was amplified from IL9 with corresponding primers Ehd5-co-F and Ehd5-co-R, and then cloned into plant binary vector pCAMBIA1301 (Cambia) using EasyGeno Assembly Cloning kit (TIANGEN). Control plants were generated by introducing the empty vector into *ehd5* mutant as well. The full-length sense or antisense cDNA of *Ehd5* was amplified using primer OE-Ehd5-F and OE-Ehd5-R, and the resulting product was cloned into the expression vector pNCGR (modified based on the pCAMBIA 1301). Similarly, the FLAG-tagged *Ehd5*, GFP-tagged *Ehd5*, mcherry-tagged *Ehd5*, and Myc-tagged *Ehd5* overexpression constructs were also generated, and those vectors were modified based on the pCAMBIA 1300 (Cambia). For gene-editing knockout, constructs of *Ehd5*, *Roc4*, and *Ghd8* via CRISPR/Cas9 were designed as previously described (Ma et al. 2015a, 2015b). The primers used are listed in Supplemental Data Set S4.

All constructs were confirmed by Sanger sequencing and introduced into *Agrobacterium tumefaciens* strain EHA105, subsequently transferred into WT or *ehd5* mutant by *Agrobacterium*-mediated transformation. More than 10 positive transgenic lines were generated when constructing overexpression and knockout materials. Heading date and other agronomic traits were investigated in the T₂ generation of transgenic rice plants.

Scanning electron microscopy

About 20 mature rice seeds of each line were put into a beaker, washed with ultrasonic wave for 15 min, and cleaned with sterile water 2 to 3 times to remove epidermal hairs and dust. The rice samples were dried, fixed to the brass table, and coated with a gold sputter. For the observation of

glume cells, the samples prepared were scanned and photographed by scanning electron microscope (JSM-6360LV), and then cell number and size were counted.

RNA isolation and quantification of gene expression

For RNA extraction, WT and *ehd5* mutant plants were grown in both ASD and ALD conditions. Total RNA from the leaf, root, SAM, stem, and sheath of WT and *ehd5* mutant was isolated using the Trizol reagent (Invitrogen) according to the manufacturer’s instructions. The first-strand cDNA was synthesized from 1 mg of total RNA using ReverTra Ace qPCR RT Master Mix with gDNA Remover (Toyobo). RT-qPCR analysis was performed using THUNDERBIRD SYBR qPCR Master Mix (Toyobo) with the Applied Biosystems QuantStudio 5 PCR system according to the manufacturer’s instructions. The cycling conditions included incubation for 60 s at 95 °C followed by 40 cycles of amplification (95 °C for 15 s and 60 °C for 60 s) and rice gene *UBQ5* (*Os01g0328400*) was used as an endogenous control. Three independent biological replicates were conducted for each sample. Each biological replicate involved the growth and treatment of a distinct group of plants under the same experimental conditions. Three times technical replicates were performed within each biological replicate. The final results were obtained by selecting the technically replicated measurements with the most accurate and consistent outcomes from the three biological replicates.

The primers used for RT-qPCR are listed in Supplemental Data Set S4.

Transcriptome sequencing and data analysis

A total of 52 leaf samples, with 26 samples collected from WT plants and 26 samples from *ehd5* mutant plants, were obtained every four hours from 33-d-old plants grown under both ASD and ALD conditions for 48 h. Total RNA was extracted from each leaf sample and subjected to transcriptome sequencing with paired-end 150 bp protocol on Illumina HiSeq2500 sequencing platform. The RNA-seq reads were processed using fastp (version 0.12.6) with parameters: -q 25 -l 75 to remove adapters and trim low-quality bases. After quality control, 402.04 Gb clean data were kept for the following analysis. We mapped the RNA-seq reads to rice reference genome (MSU v7) using HISAT2 software (version 2.0.4) with default parameters. Transcript expression levels for each sample were calculated using Cuffquant, which is part of the Cufflinks software package. The expression data were then normalized across all samples using Cuffnorm, which employs fragments per kilobase of exon per million fragments mapped (FPKM) as a normalization method to compare expression data across different samples. The resulting FPKM expression profiles of all 52 samples were used to perform WGCNA using the R package WGCNA. Firstly, we calculated the median absolute deviation (MAD) for each gene across all samples and ranked the genes in decreasing order based on their MAD values. The top 20,000 genes by MAD were retained for subsequent analysis. The “blockwiseModules” function

within WGCNA was used to construct networks and detect modules using modified parameters, including `maxBlockSize = 10000`, `TOMType = "unsigned"`, `minModuleSize = 30`, `reassignThreshold = 0`, `mergeCutHeight = 0.25`, `numericLabels = TRUE`, and `pamRespectsDendro = FALSE`. The best beta value required by the "blockwiseModules" function was selected using the "pickSoftThreshold" function. GO enrichment analysis was conducted using agriGO v2.0 on the genes contained within each module (Tian et al. 2017). The statistical method employed was Fisher, and the multitest adjustment method used was Hochberg (false discovery rate), with a significance level of 0.05. The visualization of GO enrichment was conducted using R package ggplot2. Additionally, we conducted descriptive and correlational analyses of the expression levels of different flowering-related genes using R packages base (version 3.8.5) and corplot (version 0.92), respectively. To investigate the roles of Ehd5 in the regulatory network of flowering time, gene expression analysis of both WT and ehd5 mutant plants was performed using RNA-Seq.

Phylogenetic analysis

We searched and downloaded rice *Ehd5* homologous genes in other species from Phytozome database. The coding sequences (CDS) of *Ehd5* and its homologs in selected plant species were aligned using multiple alignment using fast fourier transform software with `-auto` option. The aligned CDS were then used to construct a neighbor-joining phylogenetic tree using MEGA X with 1,000 bootstrap replicates.

We also obtained Ehd5 sequences from 162 divergent accessions in the Rice pan-genome dataset generated by our lab by performing a blast Search. Multiple sequence alignment was performed using the Clustal W program. The aligned sequences were used to construct a phylogenetic tree using the neighbor-joining method with 1,000 bootstrap replicates in MEGA X.

Alignment and machine-readable tree files are provided as [Supplemental Files 1 to 4](#).

Preparation of rice protoplasts and subcellular localization

Approximately 80 rice seedlings of cv. GL4 that were grown for 12 d at 28 °C were harvested within 30 mins and placed in the enzymatic hydrolysate (10 mM MES [pH 5.7], 0.6 M mannitol, 10 mM CaCl₂, 0.1% (w/v) bovine serum albumin, 1.5% (w/v) Cellulase RS, and 0.75% (w/v) Macerozyme R10) for 4 h with gentle shaking at 25 °C for purpose of isolating the protoplasts. This enzymic reaction was terminated by W5 solution (154 mM NaCl, 2 mM MES [pH 5.7], 5 mM KCl, and 125 mM CaCl₂), and then protoplasts were passed through a 40 μm cell strainer, collected via centrifugation at 100 g for 3 min, and resuspended in mannitol magnesium chloride solution (0.5 M mannitol, 15 mM MgCl₂, and 0.2 M MES [pH 5.7]).

To identify subcellular localization, the full-length coding sequence of *Ehd5* from IL9 gDNA was amplified and cloned into the vector pA7-GFP between the 35S promoter and

nopaline synthase terminator (Zhou et al. 2009). The plasmids pA7-GFP and Ehd5-GFP were transformed respectively into rice protoplasts mediated by PEG solution (40% (w/v) polyethylene glycol 4000, 100 mM CaCl₂, and 0.6 M mannitol). After incubation for 14 to 16 h at 26 °C in the dark, GFP fluorescence signal was examined using a confocal laser scanning microscope (ZEISS, LSM880). GFP signals were excited at 488 nm and optimally detected at 510 nm with a lasers value of approximately 2% and a master gain value of around 650.

Transient expression in *N. benthamiana* Leaves and BiFC Assays, LCI Assays

For BiFC assays, the ORF of *Ehd5*, *Ghd8*, and *Roc4* were amplified by using specific primers (Supplemental Data Set S4) and cloned into pL31-nYFP and pL31-cYFP vectors, respectively (Li et al. 2012). For LCI assays, the full length of *Ehd5*, *Ghd7*, and *Roc4* were amplified by using specific primers (Supplemental Data Set S4) and introduced to C-terminal fragment of luciferase (cLUC) to form cLUC-Ehd5, cLUC-Ghd7, cLUC-Roc4 (BioVector NTCC). The CDS of *Ehd5* and *Ghd8* were amplified and cloned into N-terminal fragment of luciferase (nLUC) to form nLUC-Ehd5, nLUC-Ghd8 (BioVector NTCC). The recombinant vectors were transformed into *A. tumefaciens* GV3101 (pSoup-p19), and the positive clones were grown overnight in 10 mL of medium with kanamycin. These cells were collected and resuspended in a transfer solution (10 mM MES [pH5.7], 10 mM MgCl₂, 150 μM Acetosyringone) for 4 h and then co-transformed into the leaves of 4-wk-old *Nicotiana benthamiana* plants. YFP fluorescence signals were examined using a confocal laser scanning microscope (ZEISS, LSM880). YFP signals were excited at 514 nm and optimally detected at 520 to 570 nm with a lasers value of approximately 8% and a master gain value of around 700. Luciferase signals were detected using the Tanon-5200 M image system after the sample leaves were injected with 1× luciferin.

Yeast two-hybrid assays

For yeast 2-hybrid assays, The CDS of *Ehd5* and *Roc4* were cloned into the bait vector pGBKT7 (Clontech) and prey vector pGADT7 (Clontech), respectively, to generate the binding domain fusion vectors and GAL4 activation domain (GAD). The constructs pGBKT7-*Ehd5* and pGBKT7-*Roc4* were transformed separately into the yeast (*Saccharomyces cerevisiae*) strain Y2HGold with pGADT7 to detect autoactivation. According to the manufacturer's instructions (Clontech), the 2 constructs to be validated were co-transformed into Y2HGold, as well as pGBKT7 and pGADT7 used as negative control. The yeast cells were cultured on synthetic dropout medium (SD/-Trp/-Leu, SD/-Trp/-Leu/-His, SD/-Trp/-Leu/-His/-Ade) and incubated at 30 °C for 3 to 4 d. The results were confirmed by the yeast growth status and β-galactosidase assays.

Co-immunoprecipitation

For the Co-IP assay, The CDS of *Ehd5* was fused to pNCGR-HA vector. The CDS of *Roc4* or *Ghd8* was inserted

into pCAMBIA1300-Flag vector. The plasmids were co-transformed into rice protoplasts. After incubating at 26 °C for 12 to 16 h, the transfected protoplasts were harvested by centrifugation at 300 g for 5 min. Total protein was extracted from the transfected protoplasts using immunoprecipitation buffer (25 mM Tris–HCl [pH 7.5], 150 mM NaCl, 10% (v/v) glycerol, 1 mM EDTA, 0.1% (v/v) Triton X-100, 1 mM DTT, and 1× complete protease inhibitor cocktail [Sangon Biotech]) by incubating at 4 °C for 30 min with rotation. The lysate was centrifuged at 15,000 × g for 10 min at 4 °C and the supernatant was incubated with FLAG-beads (Millipore, cat. no. A2220) for 2 h at 4 °C. The beads were collected by centrifugation at 300 × g for 2 min at 4 °C, and then washed three times with ice-cold IP buffer. The proteins were eluted from the beads by boiling in an SDS loading buffer for 5 min and analyzed by immunoblotting. Mouse anti-HA monoclonal antibody (Sigma, cat. no. H3663) was used at a 1:5000 dilution and mouse anti-FLAG monoclonal antibody (Sigma, cat. no. A8592) was used at a 1:5000 dilution.

Histochemical GUS staining

To construct promoter-GUS transgenic lines, *ProEhd5:GUS* plasmid was generated by amplifying the promoter of *Ehd5* using primers Ehd5P-F and Ehd5P-R and cloning into the pCAMBIA1301. Then the vectors were transferred into WT IL9 and *ehd5* mutant. According to the manufacturer's instructions (MaoKang, MM1001-1KIT), different tissues of the *ProEhd5:GUS* transgenic plants were placed in β-GUS staining solution, overnight at 37 °C, and then eluted in 75% ethanol several times. The GUS signals were observed under ZEISS Axio Imager and AxioCam 305 color.

Accession numbers

The sequence data from this article can be found in China Rice Data Center website (<http://www.ricedata.cn/gene/>) under the following accession numbers: *Ehd5* (LOC_Os08g38570), *Ghd8* (LOC_Os08g07740), *Roc4* (LOC_Os04g48070), *Ghd7* (LOC_Os07g15770), *Hd1* (LOC_Os06g16370), *Ehd1* (LOC_Os10g32600), *Hd3a* (LOC_Os06g06320), *RFT1* (LOC_Os06g06300).

Acknowledgments

We thank Prof. Yongzhong Xing from the National Key Laboratory of Crop Genetic Improvement, Huazhong Agricultural University, for providing the *Ghd7* seeds. We thank Prof. Hongxuan Lin from CAS Center of Excellence in Molecular Plant Sciences, Institute of Plant Physiology and Ecology for consulting on experiment design. We thank Prof. Ertao Wang, Dr. Hao Yang, and Dr. Wentao Dong from CAS Center of Excellence in Molecular Plant Sciences, Institute of Plant Physiology and Ecology for the Y3H assay and pull-down assay. We thank all colleagues from the National Center for Gene Research, CAS Center of Excellence in Molecular Plant Sciences, Institute of Plant Physiology and Ecology for their useful help.

Author contributions

Q.F., Z.-X.W., and B.H. conceived the project and its components. X.Z., Q.F., and B.H. designed the studies and experiments. X.Z. and Q.F. performed the experiments. X.Z., J.Z., and Y.-Y.S.-G. performed the genetic transformation. C.Z., D.F., Y.L., Q.T., W.L., Q.W., and J.C. performed DNA and RNA preparation for genome and transcriptome sequencing. Y.W., Q.Z., Z.-Q.W., and A.W. performed field phenotyping. L.Z. performed sequencing data preprocessing. J.M., S.T., and X.H. performed genome data analysis and transcriptome analyses. L.S. consulted the experiments. T.H. provided IT support. Z.-X.W. supplied the mutant and WT rice materials. X.Z., Q.F., and B.H. analyzed the data and wrote the manuscript.

Supplemental data

The following materials are available in the online version of this article.

Supplemental Figure S1. The *ehd5* mutants delay rice flowering and affect the main panicle size.

Supplemental Figure S2. Phenotypes and agronomic traits statistics of WT, *ehd5*, *Ehd5-CP/ehd5*, *Ehd5-OE*, and *Ehd5-OE/ehd5* plants under NSD and NLD conditions.

Supplemental Figure S3. *Ehd5* affects grain morphology by regulating cell number.

Supplemental Figure S4. Mature grain shape of the WT, *ehd5*, *Ehd5-CP/ehd5*, *Ehd5-OE*, and *Ehd5-OE/ehd5* lines.

Supplemental Figure S5. Subcellular localization and sequence alignments of *Ehd5*.

Supplemental Figure S6. Phylogenetic analysis and allele frequency of *Ehd5*.

Supplemental Figure S7. Sample clustering and Module-trait relationships.

Supplemental Figure S8. β-GUS staining in different organs in the *ProEhd5:GUS* transgenic plants.

Supplemental Figure S9. Schematic representation of *roc4* and *ehd5 roc4* mutants generated by a CRISPR/Cas9 genome-editing approach.

Supplemental Figure S10. Correlation analyses and transcript levels of different flowering-related genes.

Supplemental Figure S11. Diurnal expression of *Ghd7* and *Ehd5* in different lines under ASD and ALD conditions.

Supplemental Figure S12. CRISPR/Cas9-mediated targeted mutagenesis of *Ghd8* and diurnal expression analysis.

Supplemental Figure S13. Subcellular localization and co-expression of mCherry-*Ehd5*, *Ghd8*-GFP and mCherry-*Roc4* fusion proteins in *N. benthamiana* leaves.

Supplemental Figure S14. Phenotypic evaluation of WT, *ehd5*, and *Ehd5-CP/ehd5* plants for rice blast resistance.

Supplemental Figure S15. Predicted structures of *Ehd5* and *ehd5*.

Supplemental Data Set S1. SNPs in 3k groups. SNP-seek of *Ehd5* was performed using the rice 3k groups. 15 SNPs were found and a total of 3 haplotypes were generated.

Supplemental Data Set S2. Gene expression in IL9 and *ehd5* plants. A total of 52 RNA-seq datasets obtained from 33-d-old leaves from WT and *ehd5*. The relative expression levels of over 30,000 rice genes have been listed for each sample.

Supplemental Data Set S3. Results of statistical analysis.

Supplemental Data Set S4. Primers were used in this study.

Supplemental File 1. Machine-readable tree file for Fig. 4.

Supplemental File 2. Sequence alignment is used for phylogenetic analysis in Fig. 4.

Supplemental File 3. Machine-readable tree file for Supplemental Fig. S6.

Supplemental File 4. Sequence alignment used for phylogenetic analysis in Supplemental Fig. S6.

Funding

This work was supported by grants from the Chinese Academy of Sciences (Grant No. XDB27010301 to B.H.) and the National Natural Science Foundation of China (Grant No. 31471463 to Q.F.) and Shanghai Agriculture Applied Technology Development Program, China (Grant No. X20190103 to Q.F.).

Conflict of interest statement. The authors declare that they have no conflict of interests.

References

- Ang C, Ding Y, Zhang X, Wang C, Mou Z. Elongator plays a positive role in exogenous NAD-induced defense responses in Arabidopsis. *Mol Plant Microbe Interact.* 2016;**29**(5):396–404. <https://doi.org/10.1094/MPMI-01-16-0005-R>
- Ang C, Wang C, Mou Z. The Arabidopsis elongator complex is required for nonhost resistance against the bacterial pathogens *Xanthomonas citri* subsp. *citri* and *Pseudomonas syringae* pv. *phaseolicola* NPS3121. *New Phytol.* 2017;**214**(3):1245–1259. <https://doi.org/10.1111/nph.14442>
- Cai M, Chen S, Wu M, Zheng T, Zhou L, Li C, Zhang H, Wang J, Xu X, Chai J, et al. Early heading 7 interacts with DTH8, and regulates flowering time in rice. *Plant Cell Rep.* 2019;**38**(5):521–532. <https://doi.org/10.1007/s00299-019-02380-7>
- Dai X, Ding Y, Tan L, Fu Y, Liu F, Zhu Z, Sun X, Sun X, Gu P, Cai H, et al. *LHD1*, An allele of *DTH8/Ghd8*, controls late heading date in common wild rice (*Oryza rufipogon*). *J Integr Plant Biol.* 2012;**54**(10):790–799. <https://doi.org/10.1111/j.1744-7909.2012.01166.x>
- Dalwadi U, Yip CK. Structural insights into the function of elongator. *Cell Mol Life Sci.* 2018;**75**(9):1613–1622. <https://doi.org/10.1007/s00018-018-2747-6>
- Dauden MI, Kosinski J, Kolaj-Robin O, Desfosses A, Ori A, Faux C, Hoffmann NA, Onuma OF, Breunig KD, et al. Architecture of the yeast elongator complex. *EMBO Rep.* 2017;**18**(2):264–279. <https://doi.org/10.15252/embr.201643353>
- Doi K, Izawa T, Fuse T, Yamanouchi U, Kubo T, Shimatani Z, Yano M, Yoshimura A. *Ehd1*, a B-type response regulator in rice, confers short-day promotion of flowering and controls *FT*-like gene expression independently of *Hd1*. *Genes Dev.* 2004;**18**(8):926–936. <https://doi.org/10.1101/gad.1189604>
- Dong C, Lin Z, Diao W, Li D, Chu X, Wang Z, Zhou H, Xie Z, Shen Y, Long J. The *Elp2* subunit is essential for elongator complex assembly and functional regulation. *Structure.* 2015;**23**(6):1078–1086. <https://doi.org/10.1016/j.str.2015.03.018>
- Du A, Tian W, Wei M, Yan W, He H, Zhou D, Huang X, Li S, Ouyang X. The DTH8-Hd1 module mediates day-length-dependent regulation of rice flowering. *Mol Plant.* 2017;**10**(7):948–961. <https://doi.org/10.1016/j.molp.2017.05.006>
- Gao H, Zheng XM, Fei G, Chen J, Jin M, Ren Y, Wu W, Zhou K, Sheng P, Zhou F, et al. *Ehd4* encodes a novel and *Oryza*-genus-specific regulator of photoperiodic flowering in rice. *PLoS Genet.* 2013;**9**(2):e1003281. <https://doi.org/10.1371/journal.pgen.1003281>
- Hayama R, Izawa T, Shimamoto K. Isolation of rice genes possibly involved in the photoperiodic control of flowering by a fluorescent differential display method. *Plant Cell Physiol.* 2002;**43**(5):494–504. <https://doi.org/10.1093/pcp/pcf059>
- Hayama R, Yokoi S, Tamaki S, Yano M, Shimamoto K. Adaptation of photoperiodic control pathways produces short-day flowering in rice. *Nature.* 2003;**422**(6933):719–722. <https://doi.org/10.1038/nature01549>
- Huang X, Kurata N, Wei X, Wang ZX, Wang A, Zhao Q, Zhao Y, Liu K, Lu H, Li W, et al. A map of rice genome variation reveals the origin of cultivated rice. *Nature.* 2012;**490**(7421):497–501. <https://doi.org/10.1038/nature11532>
- Huang J, Wang MM, Bao YM, Sun SJ, Pan LJ, Zhang HS. SRWD: a novel WD40 protein subfamily regulated by salt stress in rice (*Oryzasativa*L). *Gene.* 2008;**424**(1-2):71–79. <https://doi.org/10.1016/j.gene.2008.07.027>
- Itoh H, Nonoue Y, Yano M, Izawa T. A pair of floral regulators sets critical day length for *Hd3a* florigen expression in rice. *Nat Genet.* 2010;**42**(7):635–638. <https://doi.org/10.1038/ng.606>
- Jain BP, Pandey S. WD40 repeat proteins: signalling scaffold with diverse functions. *Protein J.* 2018;**37**(5):391–406. <https://doi.org/10.1007/s10930-018-9785-7>
- Jiang P, Wang S, Jiang H, Cheng B, Wu K, Ding Y. The COMPASS-like Complex promotes flowering and panicle branching in rice. *Plant Physiol.* 2018;**176**(4):2761–2771. <https://doi.org/10.1104/pp.17.01749>
- Jung C, Müller AE. Flowering time control and applications in plant breeding. *Trends Plant Sci.* 2009;**14**(10):563–573. <https://doi.org/10.1016/j.tplants.2009.07.005>
- Kojima S, Takahashi Y, Kobayashi Y, Monna L, Sasaki T, Araki T, Yano M. *Hd3a*, a rice ortholog of the *Arabidopsis FT* gene, promotes transition to flowering downstream of *Hd1* under short-day conditions. *Plant Cell Physiol.* 2002;**43**(10):1096–1105. <https://doi.org/10.1093/pcp/pcf156>
- Komiya R, Ikegami A, Tamaki S, Yokoi S, Shimamoto K. *Hd3a* and *RFT1* are essential for flowering in rice. *Development.* 2008;**135**(4):767–774. <https://doi.org/10.1242/dev.008631>
- Kozarewa I, Turner DJ. Amplification-free library preparation for paired-end illumina sequencing. *Methods Mol Biol.* 2011;**733**:257–266. https://doi.org/10.1007/978-1-61779-089-8_18
- Li X, Liu H, Wang M, Liu H, Tian X, Zhou W, Lü T, Wang Z, Chu C, Fang J, et al. Combinations of *Hd2* and *Hd4* genes determine rice adaptability to Heilongjiang Province, northern limit of China. *J Integr Plant Biol.* 2015;**57**(8):698–707. <https://doi.org/10.1111/jipb.12326>
- Li Y, Pi L, Huang H, Xu L. ATH1 And KNAT2 proteins act together in regulation of plant inflorescence architecture. *J Exp Bot.* 2012;**63**(3):1423–1433. <https://doi.org/10.1093/jxb/err376>
- Ma H, Naseri A, Reyes-Gutierrez P, Wolfe SA, Zhang S, Pederson T. Multicolor CRISPR labeling of chromosomal loci in human cells. *Proc Natl Acad Sci U S A.* 2015a;**112**(10):3002–3007. <https://doi.org/10.1073/pnas.1420024112>
- Ma X, Zhang Q, Zhu Q, Liu W, Chen Y, Qiu R, Wang B, Yang Z, Li H, Lin Y, et al. A robust CRISPR/cas9 system for convenient, high-efficiency Multiplex genome editing in monocot and dicot plants. *Mol Plant.* 2015b;**8**(8):1274–1284. <https://doi.org/10.1016/j.molp.2015.04.007>
- Matsubara K, Yamanouchi U, Nonoue Y, Sugimoto K, Wang ZX, Minobe Y, Yano M. *Ehd3*, encoding a plant homeodomain finger-

- containing protein, is a critical promoter of rice flowering. *Plant J.* 2011;**66**(4):603–612. <https://doi.org/10.1111/j.1365-313X.2011.04517.x>
- Matsubara K, Yamanouchi U, Wang ZX, Minobe Y, Izawa T, Yano M.** Ehd2, a rice ortholog of the maize INDETERMINATE1 gene, promotes flowering by up-regulating Ehd1. *Plant Physiol.* 2008;**148**(3):1425–1435. <https://doi.org/10.1104/pp.108.125542>
- Migliori V, Mapelli M, Guccione E.** On WD40 proteins: propelling our knowledge of transcriptional control? *Epigenetics.* 2012;**7**(8):815–822. <https://doi.org/10.4161/epi.21140>
- Nemoto Y, Nonoue Y, Yano M, Izawa T.** *Hd1*, a *CONSTANS* ortholog in rice, functions as an *Ehd1* repressor through interaction with monocot-specific CCT-domain protein *Ghd7*. *Plant J.* 2016;**86**(3):221–233. <https://doi.org/10.1111/tpj.13168>
- Schapira M, Tyers M, Torrent M, Arrowsmith CH.** WD40 Repeat domain proteins: a novel target class? *Nat Rev Drug Discov.* 2017;**16**(11):773–786. <https://doi.org/10.1038/nrd.2017.179>
- Simpson GG, Dean C.** *Arabidopsis*, the Rosetta stone of flowering time? *Science.* 2002;**296**(5566):285–289. <https://doi.org/10.1126/science.296.5566.285>
- Sun K, Huang M, Zong W, Xiao D, Lei C, Luo Y, Song Y, Li S, Hao Y, Luo W, et al.** *Hd1*, *Ghd7*, and *DTH8* synergistically determine the rice heading date and yield-related agronomic traits. *J Genet Genomics.* 2022;**49**(5):437–447. <https://doi.org/10.1016/j.jgg.2022.02.018>
- Tian T, Liu Y, Yan H, You Q, Yi X, Du Z, Xu W, Su Z.** AgriGO v2.0: a GO analysis toolkit for the agricultural community, 2017 update. *Nucleic Acids Res.* 2017;**45**(W1):W122–W129. <https://doi.org/10.1093/nar/gkx382>
- Wang Y, An C, Zhang X, Yao J, Zhang Y, Sun Y, Yu F, Amador DM, Mou Z.** The Arabidopsis elongator complex subunit2 epigenetically regulates plant immune responses. *Plant Cell.* 2013b;**25**(2):762–776. <https://doi.org/10.1105/tpc.113.109116>
- Wang C, Ding Y, Yao J, Zhang Y, Sun Y, Colee J, Mou Z.** Arabidopsis elongator subunit 2 positively contributes to resistance to the necrotrophic fungal pathogens *Botrytis cinerea* and *Alternaria brassicicola*. *Plant J.* 2015;**83**(6):1019–1033. <https://doi.org/10.1111/tpj.12946>
- Wang P, Gong R, Yang Y, Yu S.** *Ghd8* controls rice photoperiod sensitivity by forming a complex that interacts with *Ghd7*. *BMC Plant Biol.* 2019b;**19**(1):462. <https://doi.org/10.1186/s12870-019-2053-y>
- Wang C, Tang S, Zhan Q, Hou Q, Zhao Y, Zhao Q, Feng Q, Zhou C, Lyu D, Cui L, et al.** Dissecting a heterotic gene through GradedPool-seq mapping informs a rice-improvement strategy. *Nat Commun.* 2019a;**10**(1):2982. <https://doi.org/10.1038/s41467-019-11017-y>
- Wei J, Choi H, Jin P, Wu Y, Yoon J, Lee YS, Quan T, An G.** *GL2*-type Homeobox gene *Roc4* in rice promotes flowering time preferentially under long days by repressing *Ghd7*. *Plant Sci.* 2016;**252**:133–143. <https://doi.org/10.1016/j.plantsci.2016.07.012>
- Wei X, Xu J, Guo H, Jiang L, Chen S, Yu C, Zhou Z, Hu P, Zhai H, Wan J.** *DTH8* Suppresses flowering in rice, influencing plant height and yield potential simultaneously. *Plant Physiol.* 2010;**153**(4):1747–1758. <https://doi.org/10.1104/pp.110.156943>
- Xue W, Xing Y, Weng X, Zhao Y, Tang W, Wang L, Zhou H, Yu S, Xu C, Li X, et al.** Natural variation in *Ghd7* is an important regulator of heading date and yield potential in rice. *Nat Genet.* 2008;**40**(6):761–767. <https://doi.org/10.1038/ng.143>
- Yan WH, Wang P, Chen HX, Zhou HJ, Li QP, Wang CR, Ding ZH, Zhang YS, Yu SB, Xing YZ, et al.** A major QTL, *Ghd8*, plays pleiotropic roles in regulating grain productivity, plant height, and heading date in rice. *Mol Plant.* 2011;**4**(2):319–330. <https://doi.org/10.1093/mp/ssq070>
- Yano M, Katayose Y, Ashikari M, Yamanouchi U, Monna L, Fuse T, Baba T, Yamamoto K, Umehara Y, Nagamura Y, et al.** *Hd1*, a major photoperiod sensitivity quantitative trait locus in rice, is closely related to the Arabidopsis flowering time gene *CONSTANS*. *Plant Cell.* 2000;**12**(12):2473–2484. <https://doi.org/10.1105/tpc.12.12.2473>
- Yano M, Sasaki T.** Genetic and molecular dissection of quantitative traits in rice. *Plant Mol. Biol.* 1997;**35**(1/2):145–153. <https://doi.org/10.1023/A:1005764209331>
- Zhang Z, Hu W, Shen G, Liu H, Hu Y, Zhou X, Liu T, Xing Y.** Alternative functions of *Hd1* in repressing or promoting heading are determined by *Ghd7* status under long-day conditions. *Sci Rep.* 2017;**7**(1):5388. <https://doi.org/10.1038/s41598-017-05873-1>
- Zhang B, Liu H, Qi F, Zhang Z, Li Q, Han Z, Xing Y.** Genetic interactions among *Ghd7*, *Ghd8*, *OsPRR37* and *Hd1* contribute to large variation in heading date in rice. *Rice.* 2019a;**12**(1):48. <https://doi.org/10.1186/s12284-019-0314-x>
- Zhang Z, Zhang B, Qi F, Wu H, Li Z, Xing Y.** *Hd1* function conversion in regulating heading is dependent on gene combinations of *Ghd7*, *Ghd8*, and *Ghd7.1* under long-day conditions in rice. *Mol Breed.* 2019b;**39**(7). <https://doi.org/10.1007/s11032-019-1001-8>
- Zhang J, Zhou X, Yan W, Zhang Z, Lu Li, Han Zhongmin, Zhao Hu, Liu H, Song P, Hu Y, et al.** Combinations of the *Ghd7*, *Ghd8* and *Hd1* genes largely define the ecogeographical adaptation and yield potential of cultivated rice. *New Phytol.* 2015;**208**(4):1056–1066. <https://doi.org/10.1111/nph.13538>
- Zhao J, Chen H, Ren D, Tang H, Qiu R, Feng J, Long Y, Niu B, Chen D, Zhong T, et al.** Genetic interactions between diverged alleles of *Early heading date 1 (Ehd1)* and *Heading date 3a (Hd3a)/RICE FLOWERING LOCUS T1 (RFT1)* control differential heading and contribute to regional adaptation in rice (*Oryza sativa*). *New Phytol.* 2015;**208**(3):936–948. <https://doi.org/10.1111/nph.13503>
- Zhao Q, Feng Q, Lu H, Li Y, Wang A, Tian Q, Zhan Q, Lu Y, Zhang L, Huang T, et al.** Pan-genome analysis highlights the extent of genomic variation in cultivated and wild rice. *Nat Genet.* 2018;**50**(2):278–284. <https://doi.org/10.1038/s41588-018-0041-z>
- Zhou B, Zhao X, Kawabata S, Li Y.** Transient expression of a foreign gene by direct incorporation of DNA into intact plant tissue through vacuum infiltration. *Biotechnol Lett.* 2009;**31**(11):1811–1815. <https://doi.org/10.1007/s10529-009-0080-8>
- Zhou S, Zhu S, Cui S, Hou H, Wu H, Hao B, Cai L, Xu Z, Liu L, Jiang L, et al.** Transcriptional and post-transcriptional regulation of heading date in rice. *New Phytol.* 2021;**230**(3):943–956. <https://doi.org/10.1111/nph.17158>
- Zhu S, Wang J, Cai M, Zhang H, Wu F, Xu Y, Li C, Cheng Z, Zhang X, Guo X, et al.** The OsHAPL1-DTH8-hd1 complex functions as the transcription regulator to repress heading date in rice. *J Exp Bot.* 2017;**68**(3):553–568. <https://doi.org/10.1093/jxb/erw468>
- Zong W, Ren D, Huang M, Sun K, Feng J, Zhao J, Xiao D, Xie W, Liu S, Zhang H, et al.** Strong photoperiod sensitivity is controlled by cooperation and competition among *Hd1*, *Ghd7* and *DTH8* in rice heading. *New Phytol.* 2021;**229**(3):1635–1649. <https://doi.org/10.1111/nph.16946>